

**Titolo**

**H.B. Robinson-2 Pressure Vessel Dosimetry Benchmark: Summary of ENEA-Bologna Three-Dimensional Deterministic Analyses**

**Descrittori**

Tipologia del documento: Rapporto tecnico

Collocazione contrattuale:

Argomenti trattati: Fisica nucleare, dati Nucleari, fisica dei reattori nucleari

**Sommario**

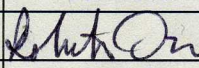
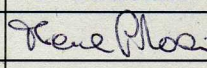
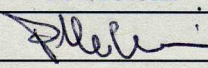
The H.B. Robinson Unit 2 (HBR-2) Pressure Vessel Dosimetry Benchmark is an in- and ex-Reactor Pressure Vessel (RPV) neutron dosimetry benchmark based on experimental data from the HBR-2 reactor, a 2300-MW PWR designed by Westinghouse and put in operation in March 1971, openly available through the SINBAD Database at OECD/NEA data Bank. The HBR-2 analysis in the SINBAD database consisted in using the two-dimensional (2D) discrete ordinates ( $S_N$ ) code DORT and the flux synthesis method. The goals of the present work were to perform three-dimensional (3D) fixed source transport calculations in both Cartesian (X,Y,Z) and cylindrical (R, $\theta$ ,Z) geometries by using the TORT-3.2 discrete ordinates code on very detailed HBR-2 3D geometrical models and to test the latest broad-group coupled (47 neutron groups + 20 photon groups) working cross section libraries in FIDO-ANISN format with same structure as BUGLE-96, such as the ENEA-Bologna BUGJEFF311.BOLIB and BUGENDF70.BOLIB libraries and the ORNL BUGLE-B7 library as well. All the cited libraries, BUGLE-96 included, were alternatively used in the calculations and the related results are here reported and compared on both (X,Y,Z) and (R, $\theta$ ,Z) geometries. **This document is a summary of the analysis thoroughly described in ENEA-Bologna SICNUC-P9H6-003** and contains some information omitted in such a report.

**Note**


Author: Roberto ORSI

**Copia n.**

**In carico a:**

2			NOME			
			FIRMA			
1			NOME			
			FIRMA			
0	EMISSIONE	25-03-2019	NOME	R. Orsi	F. Padoani	P. Meloni
			FIRMA			
REV.	DESCRIZIONE	DATA	REDAZIONE	CONVALIDA	APPROVAZIONE	



 <b>Centro Ricerche Bologna</b>	<b>Sigla di identificazione</b>	<b>Rev.</b>	<b>Distrib.</b>	<b>Pag.</b>	<b>di</b>
	SICNUC-P9H6-005	0	L	2	33

## INDEX


	Page
1. INTRODUCTION AND ANALYSIS GOALS	3
2. CROSS SECTION LIBRARIES AND NUCLEAR DATA USED IN CALCULATIONS	4
3. TRANSPORT CALCULATION GENERAL FEATURES	5
4. RESULTS	7
5. OMITTED INFORMATION IN TECHNICAL REPORT SICNUC-P9H6-003	10
6. CONCLUSIONS	10
REFERENCES	11

Tables from page. 14 to pag. 18

Figures from pag. 19 to pag. 33

## 1. INTRODUCTION AND ANALYSIS GOALS

The H.B. Robinson Unit 2 Pressure Vessel Dosimetry Benchmark /1//2/ is an in- and ex-Reactor Pressure Vessel (RPV) neutron dosimetry benchmark based on experimental data from the HBR-2 reactor, a 2300-MW PWR designed by Westinghouse, put in operation in March 1971 and owned by Carolina Power and Light Company. The HBR-2 benchmark is openly available through the SINBAD Database /3/ at OECD/NEA data Bank and, according to the U.S. Nuclear Regulatory Guide 1.190 /4/, analysis of the HBR-2 benchmark can be used as partial fulfillment of the requirements for the qualification of the methodology for calculating neutron fluence in RPVs. The specific activities at the end of fuel cycle 9 (from 21-08-1982 to 26-01-1984) of six dosimeters ( $^{237}\text{Np}(n,f)^{137}\text{Cs}$ ,  $^{238}\text{U}(n,f)^{137}\text{Cs}$ ,  $^{58}\text{Ni}(n,p)^{58}\text{Co}$ ,  $^{54}\text{Fe}(n,p)^{54}\text{Mn}$ ,  $^{46}\text{Ti}(n,p)^{46}\text{Sc}$ ,  $^{63}\text{Cu}(n,\alpha)^{60}\text{Co}$ ) are the measured (M) quantities to be compared with the calculated values (C). The main feature of the HBR-2 benchmark is that it provides measurements on both sides of the pressure vessel. In fact the dosimeters are located on the mid-plane of the HBR-2 core in the surveillance capsule, placed in the down-comer region between the thermal shield and the pressure vessel, and outside the pressure vessel, in the cavity between the vessel and the biological shield. The HBR-2 calculation methodology available in the SINBAD database consisted in using the 2D discrete ordinates ( $S_N$ ) code DORT /5/ and the flux synthesis method. A transport analysis on a detailed 3D model is without any doubt an important improvement, since reliable results can be theoretically obtained in a single run all over the model and not only in the core mid-plane. That was one of the goals of this work. Obtaining detailed HBR-2 geometrical models, up to the biological shield, both in (X,Y,Z) and (R, $\theta$ ,Z) geometries is fast and easily achievable through the ENEA-Bologna BOT3P-5.3 code system /6//7/. Moreover BOT3P permits to input the neutron source pin by pin and can automatically adapt it to the desired Cartesian or cylindrical geometry for transport calculations. Comparing the results obtained with two different geometry approaches was another aim of the analysis, as well. Finally, testing the latest broad-group coupled working cross section libraries in FIDO-ANISN format with same structure as BUGLE-96 /8/, such as the ENEA-Bologna BUGJEFF311.BOLIB /9/ and BUGENDF70.BOLIB /10/ libraries and the ORNL BUGLE-B7 /11/ library was the last but not least aim of the work. Thus, in order to achieve all these goals, 3D fixed source transport calculations in both (X,Y,Z) and (R, $\theta$ ,Z) geometries with the TORT-3.2 /12/ discrete ordinates code on very detailed 3D geometrical models were performed by alternatively using the cited working cross section libraries.

 <b>Centro Ricerche Bologna</b>	<b>Sigla di identificazione</b>	<b>Rev.</b>	<b>Distrib.</b>	<b>Pag.</b>	<b>di</b>
	SICNUC-P9H6-005	0	L	4	33

## 2. CROSS SECTION LIBRARIES AND NUCLEAR DATA USED IN CALCULATIONS

The BUGLE-96, BUGJEFF311.BOLIB, BUGENDF70.BOLIB and BUGLE-B7 group working cross section libraries were alternatively used in the present deterministic transport analysis. BUGLE-96, based on the US ENDF/B-VI.3 /13/ evaluated nuclear data library, is an international reference standard as a multi-group library for Light Water Reactor (LWR) shielding and pressure vessel dosimetry applications.

BUGJEFF311.BOLIB and BUGENDF70.BOLIB are ENEA-Bologna broad-group coupled neutron and photon working cross section libraries, generated in the same energy group structure of the ORNL BUGLE-96 library. They are based on JEFF-3.1.1 /14//15/ and US ENDF/B-VII.0 /16/ evaluated nuclear data, respectively. BUGJEFF311.BOLIB and BUGENDF70.BOLIB were obtained through problem-dependent cross section collapsing and self-shielding from the ENEA-Bologna VITJEFF311.BOLIB /17/ and VITENDF70.BOLIB /18/ fine-group coupled neutron and photon pseudo-problem-independent libraries in AMPX format, respectively. It is worth underlining that VITJEFF311.BOLIB and VITENDF70.BOLIB adopt the same energy group structure (199 neutron groups + 42 photon groups) of the ORNL VITAMIN-B6 /8/ and ORNL VITAMIN-B7 /11/ libraries and are all based on the Bondarenko /19/ (f-factor) neutron resonance self-shielding method. BUGJEFF311.BOLIB and BUGENDF70.BOLIB were generated by using the ENEA-Bologna 2007 Revision /20/ of the ORNL SCAMPI /21/ nuclear data processing system.

BUGLE-B7, an ORNL broad-group coupled neutron and photon working cross section library, was generated by using the ORNL AMPX-6 /22/ nuclear data processing system.

BUGLE-B7 is also based on the US ENDF/B-VII.0 evaluated nuclear data library as BUGENDF70.BOLIB and was obtained through problem-dependent cross section collapsing and self-shielding from VITAMIN-B7.

The fission neutron spectrum used in calculation was taken as the average of  $^{235}\text{U}$  and  $^{239}\text{Pu}$  in order to account for the contribution of  $^{235}\text{U}$  and  $^{239}\text{Pu}$  to the fission neutron source, as recommended in /1/. The fission spectra used in transport calculations for BUGJEFF311.BOLIB, BUGENDF70.BOLIB, BUGLE-B7 and BUGLE-96 are reported in Table 1. It is important to underline that BUGJEFF311.BOLIB and BUGENDF70.BOLIB include both contribution of prompt and delayed neutrons, whereas BUGLE-B7 and BUGLE-96 only of the prompt ones. Obtaining in both BUGJEFF311.BOLIB and BUGENDF70.BOLIB total fission spectra for all fissionable isotopes was made possible through the use of the ENEA-Bologna 2007 Revision of the ORNL SCAMPI nuclear data processing system.

The dosimeter cross sections used in the transport calculations were all derived from the IAEA International Reactor Dosimetry File 2002 (IRDF-2002) /23/.

The  $^{237}\text{Np}(n,f)$ ,  $^{238}\text{U}(n,f)$ ,  $^{58}\text{Ni}(n,p)$ ,  $^{58}\text{Co}$ ,  $^{54}\text{Fe}(n,p)$ ,  $^{54}\text{Mn}$ ,  $^{46}\text{Ti}(n,p)$ ,  $^{46}\text{Sc}$  and  $^{63}\text{Cu}(n,\alpha)$ ,  $^{60}\text{Co}$  dosimeter cross sections needed in the HBR-2 transport analyses were derived from the IRDF-2002 set of point-wise dosimetry cross sections through data processing /24/ with the GROUPIE program of the PREPRO 2007 /25/ nuclear data processing system into the 47-group neutron energy structure of BUGLE-96, using flat cross section weighting. Since flat weighting was adopted, the dosimeter cross sections were the same in transport calculations for all cross section libraries. The flat weighting 47-group cross sections are reported in Table 2. The  $^{237}\text{Np}(n,f)$ ,  $^{137}\text{Cs}$ ,  $^{238}\text{U}(n,f)$ ,  $^{137}\text{Cs}$  values could be obtained by multiplying the dosimeter fission cross section by the corresponding cumulative  $^{137}\text{Cs}$  fission yield for one fast fission. The following values, taken from the “Live Chart of Nuclides” of the International Atomic Energy Agency (IAEA) web site, based on JEFF-3.1.1 data, were used for all libraries in calculations:

$^{137}\text{Cs}$  fission yield in  $^{237}\text{Np} = 6.2654 \times 10^{-2}$ ;  $^{137}\text{Cs}$  fission yield in  $^{238}\text{U} = 6.0222 \times 10^{-2}$ .

### 3. TRANSPORT CALCULATION GENERAL FEATURES

Transport calculations were carried out using the TORT-3.2 3D discrete ordinates ( $S_N$ ) code included in the ORNL DOORS-3.2a /26/ system of deterministic transport codes. BUGJEFF311.BOLIB, BUGENDF70.BOLIB, ORNL BUGLE-B7 and BUGLE-96 were alternatively used in the transport calculations, performed by including all the 47 neutron energy groups. It was not possible to use the same set of atomic densities in all the calculations with all libraries, because both BUGJEFF311.BOLIB and BUGENDF70.BOLIB include all the needed processed cross sections for all the isotopes of each natural element in the HBR-2 compositional model whereas this is not always the case in both BUGLE-B7 and BUGLE-96. In fact, some needed processed cross sections are only available as natural element cross section files in BUGLE-B7 ( $\text{Ti}_{\text{nat}}$  and  $\text{Si}_{\text{nat}}$  in Inconel-718 and  $\text{Sn}_{\text{nat}}$  in Zircalloy-4) and in BUGLE-96 ( $\text{Ti}_{\text{nat}}$  and  $\text{Si}_{\text{nat}}$  in Inconel-718;  $\text{Sn}_{\text{nat}}$  in Zircalloy-4;  $\text{Si}_{\text{nat}}$ ,  $\text{Ca}_{\text{nat}}$ ,  $\text{K}_{\text{nat}}$  and  $\text{Mg}_{\text{nat}}$  in Concrete).

Both infinite dilution and self-shielded neutron cross sections were selected. Self-shielded cross sections were used when available and applicable (for example for the reactor pressure vessel, biological shield, etc.). Group-organized files of macroscopic cross sections, requested by TORT and derived from BUGJEFF311.BOLIB, BUGENDF70.BOLIB, BUGLE-B7 and BUGLE-96 in FIDO-ANISN format, were prepared through the ORNL GIP /26/ program of the DOORS system, specifically dedicated to the discrete ordinates transport codes such as TORT. The ENEA-Bologna

ADEFTA-4.1 /27/ program was employed in the calculation of the atomic densities of the isotopes involved in the compositional model on the basis of the atomic abundances reported in the BNL-NNDC database /28/. ADEFTA-4.1 was used not only to calculate the atomic densities for the benchmark experiment compositional model but also to handle them properly in order to automatically prepare the macroscopic cross section sets of the compositional model material mixtures in the format required by GIP. The automatic generation of the 3D detailed mesh grids for both Cartesian (X,Y,Z) and cylindrical (R, $\theta$ ,Z) geometries of the HBR-2 benchmark geometrical model for TORT-3.2 were performed through the ENEA-Bologna BOT3P-5.3 pre/post-processor system.

The co-ordinate origin was placed at the centre of the core mid-plane with the global Z axis normal to the core mid-plane, the X global axis in the core mid-plane, crossing the cavity where dosimeters are located ( $\theta = 0^\circ$ ), and the global Y axis normal to X in the core mid-plane. The geometrical models in calculations reproduced one quarter of the HBR-2 reactor up to the biological shield, due to symmetry conditions, with the following domains:

$$(X,Y,Z) : \quad 0. \text{ cm} \leq X \leq 348. \text{ cm}; 0. \text{ cm} \leq Y \leq 348. \text{ cm}; -213.526 \text{ cm} \leq Z \leq 212.410 \text{ cm}.$$

$$(R,\theta,Z) : \quad 0. \text{ cm} \leq R \leq 348. \text{ cm}; 0^\circ \leq \theta \leq 90^\circ; -213.526 \text{ cm} \leq Z \leq 212.410 \text{ cm}.$$

3D views of the compositional and geometrical TORT (X,Y,Z) and (R, $\theta$ ,Z) models are reported in Fig. 1 and Fig. 2, respectively.

The (X,Y,Z) and the (R, $\theta$ ,Z) models consisted of  $255X \times 240Y \times 103Z$  (= 6.303.600) and  $251R \times 215\theta \times 103Z$  (= 5.558.395) cells, respectively.

Fig. 3 and Fig. 4 show the section at  $Z=0. \text{ cm}$  (core mid-plane) of the TORT (X,Y,Z) model and of the (R, $\theta$ ,Z) one, respectively. A very little material zone exactly centered about the capsule position and another one centered about the cavity dosimeter location were introduced so as to read directly TORT results for each dosimeter as average zone results centered about the dosimeter position (see chapter 5.). Fig. 5 and Fig. 6 zoom the capsule area at the core mid-plane in the TORT (X,Y,Z) model and in the (R, $\theta$ ,Z) one, respectively.

Fixed source transport calculations with one source (outer) iteration were performed using fully symmetrical discrete ordinates directional quadrature sets for the flux solution.

The  $P_3$ - $S_8$  approximation was adopted as the standard reference, where  $P_N$  corresponds to the order of the expansion in Legendre polynomials of the scattering cross section matrix and  $S_N$  represents the order of the flux angular discretization. The theta-weighted difference approximation was selected for the flux extrapolation model. In all the calculations the same numerical value (5.E-04)

for the point-wise flux convergence criterion was employed with a maximum of 40 flux iterations per group.

The neutron source was input to the GGTM module of the BOT3P-5.3 package pin by pin and for each of the twelve axial segments of the modelled  $\frac{1}{4}$  core in accordance to the source description in /1/. GGTM automatically calculated the source density (power distribution per unit volume) for each cell of the mesh grid to be input to TORT for both (X,Y,Z) and (R, $\theta$ ,Z) geometries. The normalized power distribution (1 MW for the whole reactor, 0.25 MW for the modelled  $\frac{1}{4}$  reactor) was converted to neutrons  $s^{-1}MW^{-1}$  through a conversion factor, as reported in /1, page 27/, equal to  $8.175 \times 10^{16}$  [neutrons  $s^{-1}MW^{-1}$ ]. Fig. 7 shows the normalized power density distribution in the core mid-plane ( $Z = 0$ . cm) section of the (X,Y,Z) TORT model.

It is necessary to take into account several factors (see /1/ and /2/) in order to calculate the specific activities at the end of irradiation, which are the measured quantities provided for comparison with the calculations, such as, for example, the reactor power changes during irradiation, the closest fuel assemblies to the dosimeter locations, the different burn-up steps of fuel cycle 9. Since for each  $k^{th}$  dosimeter the calculated reaction rate  $R_{c_k}$  [ $s^{-1} \times atom^{-1}$ ] is obtained for one power distribution only (i.e., the cycle-average power distribution for the nominal core power of 2300 MW<sub>th</sub>), conversion factors  $f_k$  for each  $k^{th}$  dosimeter both in capsule and cavity locations must be calculated in order to pass from the TORT reaction rates to the measured specific activities  $A_k$  [Bq/mg], according to the following formula:  $A_k = f_k \cdot R_{c_k}$

How such conversion factors  $f_k$  were calculated, according to the guide lines contained in /1/ and in /2/, is thoroughly reported in /29/. The calculated  $f_k$  for both capsule and cavity dosimeters are summarized in Table 3.

#### 4. RESULTS

The reaction rates calculated for the cycle-average power distribution and core power of 2300 MW (100% of nominal power), using the BUGJEFF311.BOLIB, BUGENDF70.BOLIB, BUGLE-B7 and BUGLE-96 libraries in both (X,Y,Z) and (R, $\theta$ ,Z) geometries, are reported for both the surveillance capsule and the cavity dosimeter position in Table 4.

The specific activities were calculated by multiplying the conversion factors shown in Table 3 with the reaction rates in Table 4. The calculated specific activities are given in Table 5. The Measured Specific Activities, reported in /1/, are summarized in Table 6 to compare the calculated values and the experimental ones.

Ratios of Calculated to Measured (C/M) specific activities in capsule and in cavity are reported in Table 7. The results in parentheses correspond to the recommended corrections (reductions) to the experimental values (see notes in Table 1.4 in /1/) for some dosimeters, such as  $^{237}\text{Np}(n,f)^{137}\text{Cs}$ ,  $^{238}\text{U}(n,f)^{137}\text{Cs}$ ,  $^{63}\text{Cu}(n,\alpha)^{60}\text{Co}$ . According to what reported in /1/, the photo-fission contribution due to the presence of a 0.508 mm Gd cover involves in capsule estimated reductions of the measured values by 2.5% and 5% for the  $^{137}\text{Cs}$  activity in  $^{237}\text{Np}$  and  $^{238}\text{U}$ , respectively, whereas in cavity the  $^{137}\text{Cs}$  activity in  $^{237}\text{Np}$  and  $^{238}\text{U}$  should be reduced by 5.0% and 10.0%, respectively. Moreover the  $^{60}\text{Co}$  activity in  $^{63}\text{Cu}$  should be reduced by 2.5% to compensate for the contribution from the  $^{59}\text{Co}(n,\gamma)^{60}\text{Co}$  reaction on the Co impurities in the Cu dosimeter both in capsule and in cavity.

The average C/M value of all the dosimeters for each library is reported in last column of Table 7 together with its standard deviation.

The average C/M is very satisfactory for all libraries. In particular, the results for the capsule with the recommended corrections to the measured  $^{237}\text{Np}$ ,  $^{238}\text{U}$  and  $^{63}\text{Cu}$  dosimeters are:

BUGJEFF311.BOLIB	$0.97 \pm 0.09$ (X,Y,Z analysis) and $0.93 \pm 0.08$ (R, $\theta$ ,Z analysis)
BUGENDF70.BOLIB	$0.99 \pm 0.10$ (X,Y,Z analysis) and $0.95 \pm 0.09$ (R, $\theta$ ,Z analysis)
BUGLE-B7	$0.99 \pm 0.11$ (X,Y,Z analysis) and $0.95 \pm 0.10$ (R, $\theta$ ,Z analysis)
BUGLE-96	$0.94 \pm 0.08$ (X,Y,Z analysis) and $0.90 \pm 0.07$ (R, $\theta$ ,Z analysis)

In the cavity the C/M ratio for the  $^{237}\text{Np}$  dosimeter is significantly lower than C/M ratios for other dosimeters, regardless of the cross-section library used. Therefore, the average C/M values in the cavity were calculated without the  $^{237}\text{Np}$  dosimeter and that is why the related column in Table 7 is shadowed. However the obtained  $^{237}\text{Np}$  results are at least 10%-15% better than those reported in /1/. The average C/M is very satisfactory for all libraries for the cavity too. The results with recommended corrections to the measured  $^{238}\text{U}$  and  $^{63}\text{Cu}$  dosimeters are:

BUGJEFF311.BOLIB	$0.99 \pm 0.09$ (X,Y,Z analysis) and $0.99 \pm 0.08$ (R, $\theta$ ,Z analysis)
BUGENDF70.BOLIB	$1.02 \pm 0.12$ (X,Y,Z analysis) and $1.02 \pm 0.11$ (R, $\theta$ ,Z analysis)
BUGLE-B7	$1.02 \pm 0.13$ (X,Y,Z analysis) and $1.01 \pm 0.12$ (R, $\theta$ ,Z analysis)
BUGLE-96	$0.96 \pm 0.10$ (X,Y,Z analysis) and $0.95 \pm 0.09$ (R, $\theta$ ,Z analysis)



If the  $^{237}\text{Np}$  dosimeter is also taken into account in the average calculations, the cavity results are (with correction to the measured  $^{237}\text{Np}$ ,  $^{238}\text{U}$  and  $^{63}\text{Cu}$  dosimeters):

BUGJEFF311.BOLIB	$0.94 \pm 0.15$ (X,Y,Z analysis) and $0.95 \pm 0.13$ (R, $\theta$ ,Z analysis)
BUGENDF70.BOLIB	$0.97 \pm 0.17$ (X,Y,Z analysis) and $0.97 \pm 0.15$ (R, $\theta$ ,Z analysis)
BUGLE-B7	$0.96 \pm 0.19$ (X,Y,Z analysis) and $0.96 \pm 0.17$ (R, $\theta$ ,Z analysis)
BUGLE-96	$0.91 \pm 0.16$ (X,Y,Z analysis) and $0.91 \pm 0.14$ (R, $\theta$ ,Z analysis)

It can be noticed that the (R, $\theta$ ,Z) calculation results in the surveillance capsule are in average 4% lower than in the (X,Y,Z) ones for all libraries. On the contrary, this difference is at most only 1% in the cavity. In capsule, results are more affected by the fact that the (R, $\theta$ ,Z) geometry perfectly describes the reactor cylindrical components, whereas the (X,Y,Z) geometry perfectly describes the neutron source and the core baffle. Moreover, the shape and the size of the material zone with center in the dosimeter location plays a non-negligible role. It can be supposed that intermediate results between those obtained with these two geometrical approaches may reasonably be considered the most reliable ones.

BUGLE-96 systematically underestimate the results with respect to the other three more recent broad-group libraries, from 3% to 5% in capsule and from 3% to 7% in cavity.

BUGJEFF311.BOLIB performance is very satisfactory too and can be located between BUGLE-96 and BUGENDF70.BOLIB (and BUGLE-B7).

The average C/M ratios in the cavity are not very different from those in the capsule; therefore, no decrease in the C/M ratios with increasing distance from the core and increasing thickness of steel penetrated is observed. The standard deviation of the average C/M ratios is  $\sim \pm 0.10$  in the capsule and  $\sim \pm 0.11$  in the cavity for the four libraries.

Figs. 8, 9, 10 and 11 show the spatial distribution of the total neutron flux in a 3D view of the upper part of the reactor pressure vessel from the core mid-plane in the TORT-3.2 (R, $\theta$ ,Z) calculations using BUGJEFF311.BOLIB, BUGENDF70.BOLIB, BUGLE-B7 and BUGLE-96, respectively.

Very significant discrepancies were found among the different library results as for the group fluxes at low energy (below  $\sim 1$  eV), corresponding to the energy groups 45, 46 and 47.

For these low energy groups the point-wise flux convergence criterion requirements were not satisfied in TORT-3.2. These differences at low energies are not important for predicting radiation

damage in the steel specimens and reaction rates of the threshold neutron dosimeters in capsule and in cavity.

Figs. 12, 13 and 14 show the ratios of the group flux resulted by employing BUGJEFF311.BOLIB, BUGENDF70.BOLIB and BUGLE-97 to that from BUGLE-96, respectively, obtained in the TORT (R, $\theta$ ,Z) calculations in the surveillance capsule and in the cavity with energy above 1 eV. All that makes it possible a detailed comparison of the behaviour of each library with respect to BUGLE-96. Differences between BUGLE-B7 and BUGLE-96 can be noticed only at low energies (below 3-4 eV) and for high energies (above 3 MeV).

Fig. 15 shows the ratios of the group flux by using BUGENDF70.BOLIB to that from BUGLE-97 in order to evidence the behaviour differences of these two libraries, both originated from the same evaluated nuclide data file (ENDF/B-VII.0).

## 5. OMITTED INFORMATION IN TECHNICAL REPORT SICNUC-P9H6-003

Dosimeter reaction rates both in capsule and in cavity were directly taken from the TORT standard output as average zone results. In the (X,Y,Z) model the dosimeter capsule position zone, centered about the dosimeter position, was a parallelepiped with square section in the core mid-plane, with side= 0.5 cm and height= 1. cm. The cube shaped zone centered about the cavity dosimeter position had a side=1. cm. In the (R, $\theta$ ,Z) model both capsule and cavity zones were centered about the dosimeter positions and the zone volume was in both cases defined by the following co-ordinate range:  $\Delta R=0.5$  cm.,  $\Delta Z=1$  cm.,  $\Delta\theta=0.2^\circ$ .

On the contrary, flux results reported in /29/ were taken from the "VARSCS" TORT binary output file through the RVARSCS module of BOT3P-5.3 and refer to a mesh cell containing the dosimeter position, belonging to the respective capsule or cavity dosimeter zone. Thus, they are cell values and not average zone values.

## 6. CONCLUSIONS

Three-dimensional fixed source transport calculations were performed in both Cartesian and cylindrical geometries with the TORT-3.2 discrete ordinates code on detailed HBR-2 geometrical models. The results were better, that is ratios of calculated and measured results were nearer unity, than in the DORT two-dimensional analysis with the flux synthesis method.

The geometrical approach in the analysis did not play any significant role in the cavity results.

In capsule, more sensitive to the geometrical description, up to 4% differences were found between the results in the (X,Y,Z) and (R, $\theta$ ,Z) analyses.

BUGJEFF311.BOLIB, BUGENDF70.BOLIB and BUGLE-B7 gave comparable results. In fact the average of the ratios of calculated to measured activities for all the dosimeters, both in capsule and in cavity (without the  $^{237}\text{Np}$  dosimeter), approached unity with a standard deviation from the average of about 10% for all libraries. BUGLE-96 results were satisfactory too, but underestimated by 5% in both capsule and cavity with respect to those obtained with the other libraries.

All libraries and codes used in this work are available from both OECD-NEA Data Bank and ORNL-RSICC.

## REFERENCES

- /1/ I. Remec, F.B.K. Kam, H.B. Robinson-2 Pressure Vessel Benchmark, Oak Ridge National Laboratory, NUREG/CR-6453, ORNL/TM-13204, October, 1997.
- /2/ I. Remec, H.B. Robinson-2 Pressure Vessel Dosimetry Benchmark, SINBAD ABSTRACT NEA-1517/71, OECD-NEA Data Bank.
- /3/ Radiation Shielding Integral Benchmark Archive Database (SINBAD), OECD-NEA Data Bank/ORNL-RSICC, SINBAD REACTOR, NEA-1517, 2009 Edition.
- /4/ Calculational and Dosimetry Methods for Determining Pressure Vessel Neutron Fluence, U.S. Nuclear Regulatory Commission, Regulatory Guide 1.190, March 2001.
- /5/ W.A. Rhoades et al., TORT-DORT Two- and Three-Dimensional Discrete Ordinates Transport, Version 2.8.14, CCC-543, Radiation Shielding Information Center, Oak Ridge, 1994.
- /6/ R. Orsi, BOT3P Version 5.3: A Pre/Post-Processor System for Transport Analysis, ENEA-Bologna Technical Report FPN-P9H6-011, October 22, 2008.
- /7/ R. Orsi, Potential Enhanced Performances in Radiation Transport Analysis on Structured Mesh Grids Made Available by BOT3P, Nuclear Science and Engineering, Computer Code Abstract, Volume 157, pp. 110-116, 2007.
- /8/ J.E. White, D.T. Ingersoll, R.Q. Wright, H.T. Hunter, C.O. Slater, N.M. Greene, R.E. MacFarlane, R.W. Roussin, Production and Testing of the Revised VITAMIN-B6 Fine-Group and the BUGLE-96 Broad-Group Neutron/Photon Cross-Section Libraries Derived from ENDF/B-VI.3 Nuclear Data, Oak Ridge, ORNL Report ORNL-6795/R1, NUREG/CR-6214, Revision 1, January 1995.



- /9/ M. Pescarini, V. Sinitsa, R. Orsi, M. Frisoni, BUGJEFF311.BOLIB - A JEFF-3.1.1 Broad-Group Coupled (47 n + 20  $\gamma$ ) Cross Section Library in FIDO-ANISN Format for LWR Shielding and Pressure Vessel Dosimetry Applications, ENEA-Bologna Technical Report UTFISSM-P9H6-002 Revision 1, March 14, 2013.
- /10/ M. Pescarini, V. Sinitsa, R. Orsi, M. Frisoni, BUGENDF70.BOLIB - An ENDF/B-VII.0 Broad-Group Coupled (47 n + 20  $\gamma$ ) Cross Section Library in FIDO-ANISN Format for LWR Shielding and Pressure Vessel Dosimetry Applications, ENEA-Bologna Technical Report UTFISSM-P9H6-008, January 2013.
- /11/ J. M. Risner, et al., Production and Testing of the VITAMIN-B7 Fine-Group and BUGLE-B7 Broad-Group Coupled Neutron/Gamma Cross-Section Libraries Derived from ENDF/B-VII.0 Nuclear Data, Oak Ridge National Laboratory, Oak Ridge, TN 37831-6170, report NUREG/CR-7045; ORNL/TM-2011/12 (2011).
- /12/ W.A. Rhoades, D.B. Simpson, The TORT Three-Dimensional Discrete Ordinates Neutron/Photon Transport Code (TORT Version 3), Oak Ridge, ORNL Report ORNL/TM-13221, October 1997.
- /13/ P.F. Rose, ENDF/B-VI Summary Documentation, Brookhaven National Laboratory, BNL-NCS-17541 (ENDF-201) 4<sup>th</sup> Edition, October 1991.
- /14/ The JEFF-3.1.1 Nuclear Data Library, JEFF Report 22, OECD-NEA Data Bank, 2009.
- /15/ The JEFF-3.1 Nuclear Data Library, JEFF Report 21, OECD-NEA Data Bank, 2006.
- /16/ M.B. Chadwick et al., ENDF/B-VII.0: Next Generation Evaluated Nuclear Data Library for Nuclear Science and Technology, Nuclear Data Sheets, Volume 107, Number 12, pp. 2931-3060, December 2006.
- /17/ M. Pescarini, V. Sinitsa, R. Orsi, VITJEFF311.BOLIB - A JEFF-3.1.1 Multi-Group Coupled (199 n + 42  $\gamma$ ) Cross Section Library in AMPX Format for Nuclear Fission Applications, ENEA-Bologna Technical Report UTFISSM-P9H6-003, November 2011. ENEA-Bologna Technical Report UTFISSM-P9H6-003 Revision 1, March 2013.
- /18/ M. Pescarini, V. Sinitsa, R. Orsi, M. Frisoni, VITENDF70.BOLIB - An ENDF/B-VII.0 Multi-Group Coupled (199 n + 42  $\gamma$ ) Cross Section Library in AMPX Format for Nuclear Fission Applications, ENEA-Bologna Technical Report UTFISSM-P9H6-005, May 2012.
- /19/ I.I. Bondarenko, M.N. Nikolaev, L.P. Abagyan, N.O. Bazaziants, Group Constants for Nuclear Reactors Calculations, Consultants Bureau, New York, 1964.

- /20/ V. Sinita, M. Pescarini, ENEA-Bologna 2007 Revision of the SCAMPI (ORNL) Nuclear Data Processing System, ENEA-Bologna Technical Report FPN-P9H6-006, September 13, 2007.
- /21/ SCAMPI Collection of Codes for Manipulating Multigroup Cross Section Libraries in AMPX Format, ORNL, RSIC Peripheral Shielding Routine Collection PSR-352, September 1995.
- /22/ D. Wiarda, S. Goluoglu, M.E. Dunn, N.M. Green and L. M. Petrie, AMPX-6: A Modular Code System for Processing ENDF/B Evaluations, ORNL, (2014).
- /23/ O.Bersillon, L.R. Greenwood, P.J. Griffin, W. Mannhart, H.J. Nolthenius, R. Paviotti-Corcuera, K.I. Zolotarev, E.M. Zsolnay, International Reactor Dosimetry File 2002 (IRDF-2002), IAEA, Vienna, Austria, Technical Reports Series No. 452, 2006.
- /24/ R. Orsi, M. Pescarini, V. Sinita, IRDF-2002 Dosimetry Cross Section Processing in the BUGLE-96 (47 n) Neutron Group Structure Using Flat and Updated Problem Dependent Neutron Spectra, ENEA-Bologna Technical Report UTFISSM-P9H6-006, May 9, 2012.
- /25/ D.E. Cullen, PREPRO 2007: 2007 ENDF/B Pre-processing Codes (ENDF/B-VII Tested), LLNL, owned, maintained and distributed by IAEA-NDS, Vienna, Austria, IAEA Report IAEA-NDS-39, Rev. 13, March 17, 2007.
- /26/ DOORS3.2a One-, Two- and Three-Dimensional Discrete Ordinates Neutron/Photon Transport Code System, ORNL, RSIC Computer Code Collection CCC-650, August 1996.
- /27/ R. Orsi, ADEFTA Version 4.1: A Program to Calculate the Atomic Densities of a Compositional Model for Transport Analysis, ENEA-Bologna Technical Report FPN-P9H6-010, May 2008.
- /28/ J.K. Tuli, Nuclear Wallet Cards (6<sup>th</sup> Edition), National Nuclear Data Centre, Brookhaven National Laboratory, Upton, New York 11973-5000, USA, January 2000.
- /29/ R. Orsi, H.B. Robinson-2 Pressure Vessel Dosimetry Benchmark - Deterministic Analysis in Both Cartesian (X,Y,Z) and Cylindrical (R, $\theta$ ,Z) Geometries Using the TORT-3.2 3D Transport Code, the BUGJEFF311.BOLIB, BUGENDF70.BOLIB, BUGLE-B7 and the BUGLE-96 Cross Section Libraries, ENEA-Bologna Technical Report SICNUC-P9H6-003, February 2019.

**Table 1**

**Total or Prompt  $\frac{1}{2}(^{235}\text{U}+^{239}\text{Pu})$  Fission Neutron Spectra ( $\chi$ )  
in the TORT-3.2 Calculations Using the BUGJEFF311.BOLIB,  
BUGENDF70.BOLIB, BUGLE-B7 and BUGLE-96 Libraries**

Group	Upper Energy [MeV]	Total ( $\chi$ )		Prompt ( $\chi$ )	Prompt ( $\chi$ )
		BUGJEFF311.BOLIB	BUGENDF70.BOLIB	BUGLE-B7	BUGLE-96
1	1.7332e+01	6.2600e-05	6.4498e-05	6.4080e-05	5.3193e-05
2	1.4191e+01	2.4009e-04	2.4711e-04	2.4810e-04	2.1421e-04
3	1.2214e+01	1.3098e-03	1.3425e-03	1.3480e-03	1.2191e-03
4	1.0000e+01	2.8557e-03	2.8587e-03	2.8706e-03	2.7308e-03
5	8.6071e+00	6.2344e-03	6.2368e-03	6.2630e-03	6.0634e-03
6	7.4082e+00	1.7340e-02	1.7350e-02	1.7423e-02	1.7128e-02
7	6.0653e+00	3.2309e-02	3.2321e-02	3.2460e-02	3.2364e-02
8	4.9659e+00	8.3028e-02	8.2983e-02	8.3342e-02	8.4152e-02
9	3.6788e+00	7.7838e-02	7.7788e-02	7.8128e-02	7.8994e-02
10	3.0119e+00	4.4239e-02	4.4223e-02	4.4414e-02	4.4785e-02
11	2.7253e+00	4.6701e-02	4.6691e-02	4.6892e-02	4.7170e-02
12	2.4660e+00	1.9977e-02	1.9975e-02	2.0060e-02	2.0150e-02
13	2.3653e+00	4.0122e-03	4.0120e-03	4.0289e-03	4.0368e-03
14	2.3457e+00	2.4236e-02	2.4235e-02	2.4337e-02	2.4434e-02
15	2.2313e+00	7.3020e-02	7.3019e-02	7.3320e-02	7.3494e-02
16	1.9205e+00	7.1213e-02	7.1215e-02	7.1494e-02	7.1590e-02
17	1.6530e+00	8.8385e-02	8.8392e-02	8.8676e-02	8.8754e-02
18	1.3534e+00	1.1336e-01	1.1336e-01	1.1356e-01	1.1330e-01
19	1.0026e+00	6.1702e-02	6.1716e-02	6.1680e-02	6.1273e-02
20	8.2085e-01	2.6816e-02	2.6815e-02	2.6754e-02	2.6507e-02
21	7.4274e-01	4.6107e-02	4.6128e-02	4.5945e-02	4.5390e-02
22	6.0810e-01	3.7063e-02	3.7101e-02	3.6812e-02	3.6283e-02
23	4.9787e-01	4.1258e-02	4.1267e-02	4.0804e-02	4.0306e-02
24	3.6883e-01	2.1161e-02	2.1165e-02	2.0880e-02	2.0795e-02
25	2.9721e-01	2.9834e-02	2.9823e-02	2.9326e-02	2.9357e-02
26	1.8316e-01	1.5378e-02	1.5387e-02	1.5040e-02	1.5228e-02
27	1.1109e-01	7.4605e-03	7.4459e-03	7.2493e-03	7.4611e-03
28	6.7379e-02	3.5675e-03	3.5622e-03	3.4628e-03	3.5486e-03
29	4.0868e-02	1.0074e-03	1.0071e-03	9.7473e-04	9.9750e-04
30	3.1828e-02	5.8095e-04	5.7935e-04	5.5648e-04	5.6678e-04
31	2.6058e-02	1.7767e-04	1.7716e-04	1.6933e-04	1.7373e-04
32	2.4176e-02	2.0862e-04	2.0794e-04	1.9833e-04	2.0795e-04
33	2.1875e-02	5.6369e-04	5.5924e-04	5.2782e-04	5.3524e-04
34	1.5034e-02	5.0701e-04	5.0365e-04	4.7296e-04	5.0178e-04
35	7.1017e-03	1.6210e-04	1.6245e-04	1.5382e-04	1.5762e-04
36	3.3546e-03	5.3918e-05	5.4153e-05	4.9973e-05	5.2233e-05
37	1.5846e-03	2.2995e-05	2.3067e-05	1.4174e-05	2.1404e-05
38	4.5400e-04	3.0664e-06	3.0743e-06	0.	2.5992e-06
39	2.1445e-04	1.0837e-06	1.0860e-06	0.	8.4503e-07
40	1.0130e-04	4.5980e-07	4.5977e-07	0.	3.1159e-07
41	3.7266e-05	1.3907e-07	1.3920e-07	0.	6.0722e-08
42	1.0677e-05	1.9053e-08	2.1959e-08	0.	1.3585e-11
43	5.0435e-06	9.5788e-09	9.9079e-09	0.	4.1453e-12
44	1.8554e-06	2.7569e-09	2.6753e-09	0.	3.4287e-13
45	8.7643e-07	1.2484e-09	1.2038e-09	0.	0.
46	4.1399e-07	8.2184e-10	7.9541e-10	0.	0.
47	1.0000e-07	2.5500e-10	2.4960e-10	0.	0.
	1.0000e-11				



**Table 2**

**IRDF-2002 Flat Weighting Neutron Dosimeter Cross Sections [barns]**  
**Used in the TORT-3.2 Calculations with BUGJEFF311.BOLIB,**  
**BUGENDF70.BOLIB, BUGLE-B7 and BUGLE-96.**

Group	Upper Energy [Mev]	Np-237 (n, f)	U-238 (n, f)	Ni-58 (n, p)	Fe-54 (n, p)	Ti-46 (n, p)	Cu-63 (n, α)
1	1.7332e+01	2.2071e+00	1.2190e+00	2.2132e-01	2.3634e-01	1.9614e-01	3.4460e-02
2	1.4191e+01	2.1063e+00	1.0428e+00	4.4874e-01	3.9357e-01	2.8124e-01	4.6786e-02
3	1.2214e+01	2.0841e+00	9.7830e-01	6.0075e-01	4.6624e-01	2.9804e-01	3.8885e-02
4	1.0000e+01	2.1774e+00	9.8793e-01	6.3861e-01	4.8169e-01	2.6868e-01	2.6939e-02
5	8.6071e+00	2.2235e+00	9.9636e-01	6.4484e-01	4.8240e-01	2.3930e-01	1.8860e-02
6	7.4082e+00	1.9547e+00	8.6164e-01	6.2243e-01	4.7885e-01	1.8477e-01	1.0688e-02
7	6.0653e+00	1.5224e+00	5.4549e-01	5.4560e-01	4.3669e-01	9.7292e-02	3.6481e-03
8	4.9659e+00	1.5290e+00	5.5498e-01	4.0492e-01	3.1544e-01	4.0127e-02	6.1452e-04
9	3.6788e+00	1.6280e+00	5.3415e-01	2.5204e-01	1.9564e-01	5.3275e-03	4.2940e-05
10	3.0119e+00	1.6660e+00	5.3271e-01	1.6817e-01	1.3414e-01	5.7867e-04	4.6929e-06
11	2.7253e+00	1.6804e+00	5.4403e-01	1.2162e-01	7.8808e-02	7.3689e-05	1.3682e-06
12	2.4660e+00	1.6855e+00	5.4972e-01	9.3475e-02	5.6762e-02	2.1604e-05	7.4165e-07
13	2.3653e+00	1.6868e+00	5.5067e-01	8.4827e-02	5.1203e-02	1.7487e-05	4.7235e-07
14	2.3457e+00	1.6875e+00	5.5129e-01	7.5697e-02	4.5047e-02	1.2901e-05	1.7922e-07
15	2.2313e+00	1.6832e+00	5.4443e-01	5.0849e-02	2.9403e-02	1.8982e-06	0.
16	1.9205e+00	1.6656e+00	4.8376e-01	2.5952e-02	9.5530e-03	0.	0.
17	1.6530e+00	1.6260e+00	3.2313e-01	1.1677e-02	2.9684e-03	0.	0.
18	1.3534e+00	1.5299e+00	4.4018e-02	3.7988e-03	7.8514e-04	0.	0.
19	1.0026e+00	1.4011e+00	1.2809e-02	4.8761e-04	9.0118e-05	0.	0.
20	8.2085e-01	1.2445e+00	3.7983e-03	1.5596e-04	6.6796e-06	0.	0.
21	7.4274e-01	1.0224e+00	1.4955e-03	4.1887e-05	3.9326e-07	0.	0.
22	6.0810e-01	6.5194e-01	5.9988e-04	3.3813e-06	0.	0.	0.
23	4.9787e-01	2.8178e-01	2.8527e-04	2.9075e-07	0.	0.	0.
24	3.6883e-01	9.8144e-02	1.5015e-04	0.	0.	0.	0.
25	2.9721e-01	4.5283e-02	9.3264e-05	0.	0.	0.	0.
26	1.8316e-01	2.6086e-02	6.8791e-05	0.	0.	0.	0.
27	1.1109e-01	1.6780e-02	3.8553e-05	0.	0.	0.	0.
28	6.7379e-02	1.5320e-02	8.4376e-05	0.	0.	0.	0.
29	4.0868e-02	1.5819e-02	3.6056e-05	0.	0.	0.	0.
30	3.1828e-02	1.6263e-02	5.9821e-05	0.	0.	0.	0.
31	2.6058e-02	1.6493e-02	8.4858e-05	0.	0.	0.	0.
32	2.4176e-02	1.6618e-02	9.5280e-05	0.	0.	0.	0.
33	2.1875e-02	1.7580e-02	1.1676e-04	0.	0.	0.	0.
34	1.5034e-02	2.0739e-02	1.1372e-04	0.	0.	0.	0.
35	7.1017e-03	2.5089e-02	1.6682e-05	0.	0.	0.	0.
36	3.3546e-03	3.3672e-02	4.4890e-09	0.	0.	0.	0.
37	1.5846e-03	4.5093e-02	1.0089e-03	0.	0.	0.	0.
38	4.5400e-04	6.2187e-02	1.0793e-05	0.	0.	0.	0.
39	2.1445e-04	1.0463e-01	1.9529e-05	0.	0.	0.	0.
40	1.0130e-04	1.6104e-01	3.0217e-05	0.	0.	0.	0.
41	3.7266e-05	9.3968e-02	1.4925e-04	0.	0.	0.	0.
42	1.0677e-05	2.0404e-02	6.7098e-05	0.	0.	0.	0.
43	5.0435e-06	8.9537e-03	1.7685e-06	0.	0.	0.	0.
44	1.8554e-06	1.9759e-02	1.8697e-06	0.	0.	0.	0.
45	8.7643e-07	1.1841e-02	2.5136e-06	0.	0.	0.	0.
46	4.1399e-07	6.6293e-03	3.9826e-06	0.	0.	0.	0.
47	1.0000e-07	2.1237e-02	1.1744e-05	0.	0.	0.	0.
	1.0000e-11						

Table 3

Conversion Factors  $f_k$  [atom/mg] for Capsule and Cavity Locations between Specific Activity  $A_k$  [Bq/mg] and Reaction Rate  $R_{Ck}$  [ $s^{-1} \times \text{atom}^{-1}$ ] Calculated in Transport Analysis for Nominal Core Power (2300 MW<sub>th</sub>).

Dosimeter	Capsule	Cavity
$^{237}\text{Np}(n,f)^{137}\text{Cs}$	$3.082 \times 10^{15}$	$3.085 \times 10^{15}$
$^{238}\text{U}(n,f)^{137}\text{Cs}$	$2.950 \times 10^{15}$	$2.952 \times 10^{15}$
$^{58}\text{Ni}(n,p)^{58}\text{Co}$	$3.576 \times 10^{18}$	$3.844 \times 10^{18}$
$^{54}\text{Fe}(n,p)^{54}\text{Mn}$	$2.494 \times 10^{17}$	$2.558 \times 10^{17}$
$^{46}\text{Ti}(n,p)^{46}\text{Sc}$	$5.364 \times 10^{17}$	$5.737 \times 10^{17}$
$^{63}\text{Cu}(n,\alpha)^{60}\text{Co}$	$6.697 \times 10^{17}$	$6.726 \times 10^{17}$

Table 4

Reaction Rates [ $s^{-1} \times \text{atom}^{-1}$ ] Calculated for the Cycle-average Power Distribution and Core Power of 2300 MW (100% of Nominal Power) with Different Cross-section Libraries in (X,Y,Z) and (R,  $\theta$ ,Z) Geometry Transport Calculations

Capsule							
Cross-Section Library	Geom.	$^{237}\text{Np}(n,f)$	$^{238}\text{U}(n,f)$	$^{58}\text{Ni}(n,p)$	$^{54}\text{Fe}(n,p)$	$^{46}\text{Ti}(n,p)$	$^{63}\text{Cu}(n,\alpha)$
BUGJEFF311. BOLIB	XYZ	1.0059E-13	1.5124E-14	4.8904E-15	3.6065E-15	6.9322E-16	4.0956E-17
	R $\theta$ Z	9.8569E-14	1.4573E-14	4.6816E-15	3.4502E-15	6.5888E-16	3.8807E-17
BUGENDF70. BOLIB	XYZ	1.0128E-13	1.5186E-14	4.9734E-15	3.6705E-15	7.2063E-16	4.2512E-17
	R $\theta$ Z	9.9227E-14	1.4622E-14	4.7582E-15	3.5094E-15	6.8497E-16	4.0290E-17
BUGLE-B7	XYZ	9.9165E-14	1.5120E-14	4.9816E-15	3.6789E-15	7.2387E-16	4.2712E-17
	R $\theta$ Z	9.7032E-14	1.4555E-14	4.7657E-15	3.5172E-15	6.8802E-16	4.0478E-17
BUGLE-96	XYZ	9.8633E-14	1.4712E-14	4.7487E-15	3.5003E-15	6.6997E-16	3.8978E-17
	R $\theta$ Z	9.6546E-14	1.4161E-14	4.5434E-15	3.3468E-15	6.3688E-16	3.6940E-17
Cavity							
Cross-Section Library	Geom.	$^{237}\text{Np}(n,f)$	$^{238}\text{U}(n,f)$	$^{58}\text{Ni}(n,p)$	$^{54}\text{Fe}(n,p)$	$^{46}\text{Ti}(n,p)$	$^{63}\text{Cu}(n,\alpha)$
BUGJEFF311. BOLIB	XYZ	4.8295E-15	2.2299E-16	4.8567E-17	3.3910E-17	6.2947E-18	4.0754E-19
	R $\theta$ Z	5.0761E-15	2.2486E-16	4.8288E-17	3.3627E-17	6.2184E-18	4.0160E-19
BUGENDF70. BOLIB	XYZ	4.8954E-15	2.2387E-16	4.9389E-17	3.4480E-17	6.6727E-18	4.2994E-19
	R $\theta$ Z	5.1488E-15	2.2557E-16	4.9056E-17	3.4154E-17	6.5886E-18	4.2372E-19
BUGLE-B7	XYZ	4.6532E-15	2.1885E-16	4.9227E-17	3.4482E-17	6.7150E-18	4.3271E-19
	R $\theta$ Z	4.8881E-15	2.2039E-16	4.8886E-17	3.4154E-17	6.6302E-18	4.2643E-19
BUGLE-96	XYZ	4.6259E-15	2.1409E-16	4.6665E-17	3.2524E-17	6.1383E-18	3.9074E-19
	R $\theta$ Z	4.8609E-15	2.1560E-16	4.6358E-17	3.2223E-17	6.0622E-18	3.8516E-19

Table 5

Calculated Specific Activities [Bq/mg] in (X,Y,Z) and (R, θ,Z) Transport Analyses (Specific activities are given per mg of Ni, Fe, Ti, and Cu material with naturally occurring isotopic composition and per mg of <sup>237</sup>Np and <sup>238</sup>U isotopes).

Capsule							
Cross-Section Library	Geom.	<sup>237</sup> Np(n,f) <sup>137</sup> Cs	<sup>238</sup> U(n,f) <sup>137</sup> Cs	<sup>58</sup> Ni(n,p) <sup>58</sup> Co	<sup>54</sup> Fe(n,p) <sup>54</sup> Mn	<sup>46</sup> Ti(n,p) <sup>46</sup> Sc	<sup>63</sup> Cu(n,α) <sup>60</sup> Co
BUGJEFF311. BOLIB	XYZ	3.100E+02	4.462E+01	1.749E+04	8.995E+02	3.718E+02	2.743E+01
	RθZ	3.038E+02	4.299E+01	1.674E+04	8.605E+02	3.534E+02	2.599E+01
BUGENDF70. BOLIB	XYZ	3.122E+02	4.480E+01	1.778E+04	9.154E+02	3.865E+02	2.847E+01
	RθZ	3.058E+02	4.313E+01	1.702E+04	8.752E+02	3.674E+02	2.698E+01
BUGLE-B7	XYZ	3.056E+02	4.460E+01	1.781E+04	9.175E+02	3.883E+02	2.860E+01
	RθZ	2.991E+02	4.294E+01	1.704E+04	8.772E+02	3.691E+02	2.711E+01
BUGLE-96	XYZ	3.040E+02	4.340E+01	1.698E+04	8.730E+02	3.594E+02	2.610E+01
	RθZ	2.976E+02	4.177E+01	1.625E+04	8.347E+02	3.416E+02	2.474E+01
Cavity							
Cross-Section Library	Geom.	<sup>237</sup> Np(n,f) <sup>137</sup> Cs	<sup>238</sup> U(n,f) <sup>137</sup> Cs	<sup>58</sup> Ni(n,p) <sup>58</sup> Co	<sup>54</sup> Fe(n,p) <sup>54</sup> Mn	<sup>46</sup> Ti(n,p) <sup>46</sup> Sc	<sup>63</sup> Cu(n,α) <sup>60</sup> Co
BUGJEFF311. BOLIB	XYZ	1.490E+01	6.583E-01	1.867E+02	8.674	3.611	2.741E-01
	RθZ	1.566E+01	6.638E-01	1.856E+02	8.602	3.567	2.701E-01
BUGENDF70. BOLIB	XYZ	1.510E+01	6.609E-01	1.898E+02	8.820	3.828	2.892E-01
	RθZ	1.588E+01	6.659E-01	1.886E+02	8.736	3.780	2.850E-01
BUGLE-B7	XYZ	1.436E+01	6.461E-01	1.892E+02	8.821	3.852	2.910E-01
	RθZ	1.508E+01	6.506E-01	1.879E+02	8.737	3.804	2.868E-01
BUGLE-96	XYZ	1.427E+01	6.320E-01	1.794E+02	8.320	3.522	2.628E-01
	RθZ	1.500E+01	6.365E-01	1.782E+02	8.243	3.478	2.591E-01

Table 6

Measured Specific Activities [Bq/mg]

	<sup>237</sup> Np(n,f) <sup>137</sup> Cs	<sup>238</sup> U(n,f) <sup>137</sup> Cs	<sup>58</sup> Ni(n,p) <sup>58</sup> Co	<sup>54</sup> Fe(n,p) <sup>54</sup> Mn	<sup>46</sup> Ti(n,p) <sup>46</sup> Sc	<sup>63</sup> Cu(n,α) <sup>60</sup> Co
Reaction product half-life (T <sub>1/2</sub> )	30 years	30 years	71 days	313 days	84 days	5.3 years
Dosimeter Location	Measured Values and "Adjusted" Measured Values (see notes in /1/, Table 1.4)					
Capsule (measured)	3.671E+02	5.345E+01	1.786E+04	9.342E+02	3.500E+02	2.646E+01
Capsule (adjusted)	3.579E+02	5.078E+01				2.580E+01
Cavity (measured)	2.236E+01	8.513E-01	1.959E+02	8.711	3.310	2.645E-01
Cavity (adjusted)	2.124E+01	7.662E-01				2.579E-01



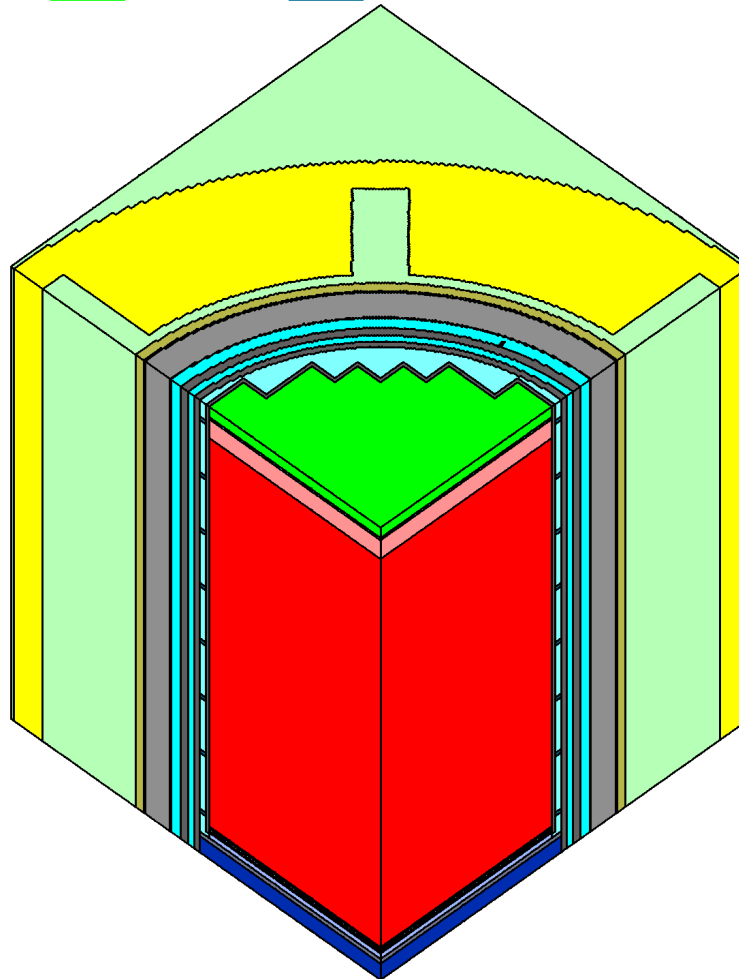
Table 7  
Ratios of Calculated to Measured (C/M) Specific Activities

Capsule								
Cross-Section Library	Geom.	$^{237}\text{Np}(n,f)$ $^{137}\text{Cs}$	$^{238}\text{U}(n,f)$ $^{137}\text{Cs}$	$^{58}\text{Ni}(n,p)$ $^{58}\text{Co}$	$^{54}\text{Fe}(n,p)$ $^{54}\text{Mn}$	$^{46}\text{Ti}(n,p)$ $^{46}\text{Sc}$	$^{63}\text{Cu}(n,\alpha)$ $^{60}\text{Co}$	Average $\pm \sigma$
BUGJEFF311. BOLIB	XYZ	0.84 (0.87)	0.83 (0.88)	0.98	0.96	1.06	1.04 (1.06)	0.95 $\pm$ 0.10 (0.97 $\pm$ 0.09)
	R0Z	0.83 (0.85)	0.80 (0.85)	0.94	0.92	1.01	0.98 (1.01)	0.91 $\pm$ 0.09 (0.93 $\pm$ 0.08)
BUGENDF70. BOLIB	XYZ	0.85 (0.87)	0.84 (0.88)	1.00	0.98	1.10	1.08 (1.10)	0.97 $\pm$ 0.11 (0.99 $\pm$ 0.10)
	R0Z	0.83 (0.85)	0.81 (0.85)	0.95	0.94	1.05	1.02 (1.05)	0.93 $\pm$ 0.10 (0.95 $\pm$ 0.09)
BUGLE-B7	XYZ	0.83 (0.85)	0.83 (0.88)	1.00	0.98	1.11	1.08 (1.11)	0.97 $\pm$ 0.12 (0.99 $\pm$ 0.11)
	R0Z	0.81 (0.84)	0.80 (0.85)	0.95	0.94	1.05	1.02 (1.05)	0.93 $\pm$ 0.11 (0.95 $\pm$ 0.10)
BUGLE-96	XYZ	0.83 (0.85)	0.81 (0.85)	0.95	0.93	1.03	0.99 (1.01)	0.92 $\pm$ 0.09 (0.94 $\pm$ 0.08)
	R0Z	0.81 (0.83)	0.78 (0.82)	0.91	0.89	0.98	0.93 (0.96)	0.88 $\pm$ 0.09 (0.90 $\pm$ 0.07)
Cavity (Average without $^{237}\text{Np}(n,f)^{137}\text{Cs}$ Dosimeter)								
Cross-Section Library	Geom.	$^{237}\text{Np}(n,f)$ $^{137}\text{Cs}$	$^{238}\text{U}(n,f)$ $^{137}\text{Cs}$	$^{58}\text{Ni}(n,p)$ $^{58}\text{Co}$	$^{54}\text{Fe}(n,p)$ $^{54}\text{Mn}$	$^{46}\text{Ti}(n,p)$ $^{46}\text{Sc}$	$^{63}\text{Cu}(n,\alpha)$ $^{60}\text{Co}$	Average $\pm \sigma$
BUGJEFF311. BOLIB	XYZ	0.67 (0.70)	0.77 (0.86)	0.95	1.00	1.09	1.04 (1.06)	0.97 $\pm$ 0.13 (0.99 $\pm$ 0.09)
	R0Z	0.70 (0.74)	0.78 (0.87)	0.95	0.99	1.08	1.02 (1.05)	0.96 $\pm$ 0.12 (0.99 $\pm$ 0.08)
BUGENDF70. BOLIB	XYZ	0.68 (0.71)	0.78 (0.86)	0.97	1.01	1.16	1.09 (1.12)	1.00 $\pm$ 0.14 (1.02 $\pm$ 0.12)
	R0Z	0.71 (0.75)	0.78 (0.87)	0.96	1.00	1.14	1.08 (1.11)	0.99 $\pm$ 0.14 (1.02 $\pm$ 0.11)
BUGLE-B7	XYZ	0.64 (0.68)	0.76 (0.84)	0.97	1.01	1.16	1.10 (1.13)	1.00 $\pm$ 0.15 (1.02 $\pm$ 0.13)
	R0Z	0.67 (0.71)	0.76 (0.85)	0.96	1.00	1.15	1.08 (1.11)	0.99 $\pm$ 0.15 (1.01 $\pm$ 0.12)
BUGLE-96	XYZ	0.64 (0.67)	0.74 (0.82)	0.92	0.96	1.06	0.99 (1.02)	0.93 $\pm$ 0.13 (0.96 $\pm$ 0.10)
	R0Z	0.67 (0.71)	0.75 (0.83)	0.91	0.95	1.05	0.98 (1.00)	0.93 $\pm$ 0.12 (0.95 $\pm$ 0.09)

Fig. 1

3D View of the Compositional and Geometrical Model in the HBR-2 TORT-3.2 (X,Y,Z) Calculations.

Core	SS-304	H2O-0.776	H2O-0.787	RPV-A533B
Insulation	Air	Concrete	Core Support	Lower Core Plate
Nozzle Legs	Bottom Nozzle Plate	Water Gap 1	End Plugs	Fuel Plenum
Water Gap 2	Top Nozzle	Formers		



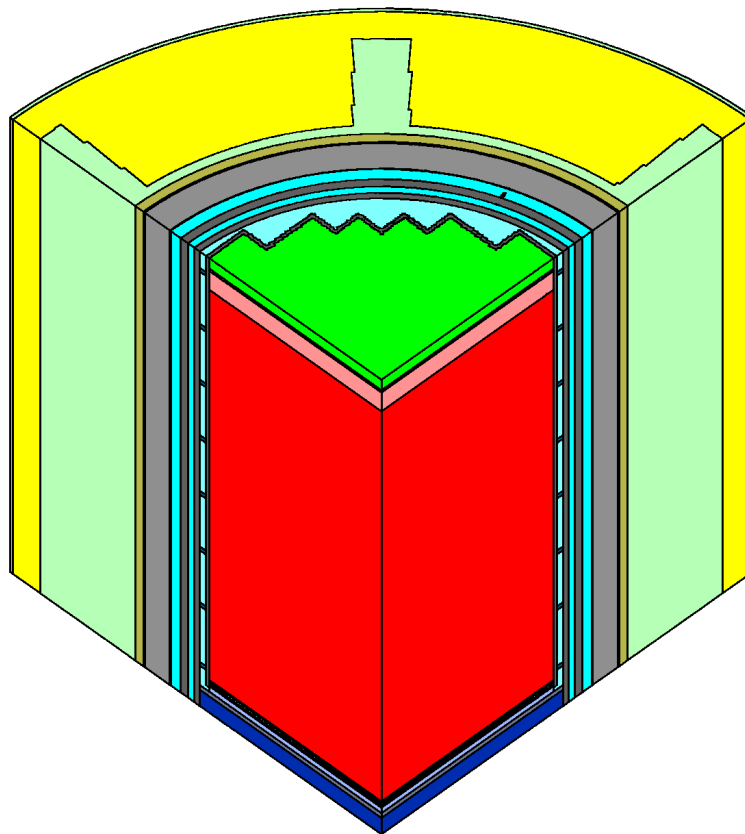
Meshes: 255X,240Y,103Z

$\alpha = 225.00$     $\omega = 45.00$     $X = (0.000E+00, 3.480E+02)$     $Y = (0.000E+00, 3.480E+02)$     $Z = (-2.135E+02, 2.124E+02)$

Fig. 2

3D View of the Compositional and Geometrical Model in the HBR-2 TORT-3.2 (R,θ,Z) Calculations.

Core	SS-304	H2O-0.776	H2O-0.787	RPV-A533B
Insulation	Air	Concrete	Core Support	Lower Core Plate
Nozzle Legs	Bottom Nozzle Plate	Water Gap 1	End Plugs	Fuel Plenum
Water Gap 2	Top Nozzle	Formers		



Meshes: 251R,215θ,103Z

$\alpha = 225.00$     $\omega = 45.00$     $R = (0.000E+00, 3.480E+02)$     $\theta = (0.000E+00, 9.000E+01)$     $Z = (-2.135E+02, 2.124E+02)$

Fig. 3

Compositional and Geometrical Model in the HBR-2 TORT-3.2 (X,Y,Z) Calculations.  
Section at the Core Mid-Plane (Z = 0. cm)  
Dosimeter Locations "x", 255X×240Y×103Z Spatial Meshes.

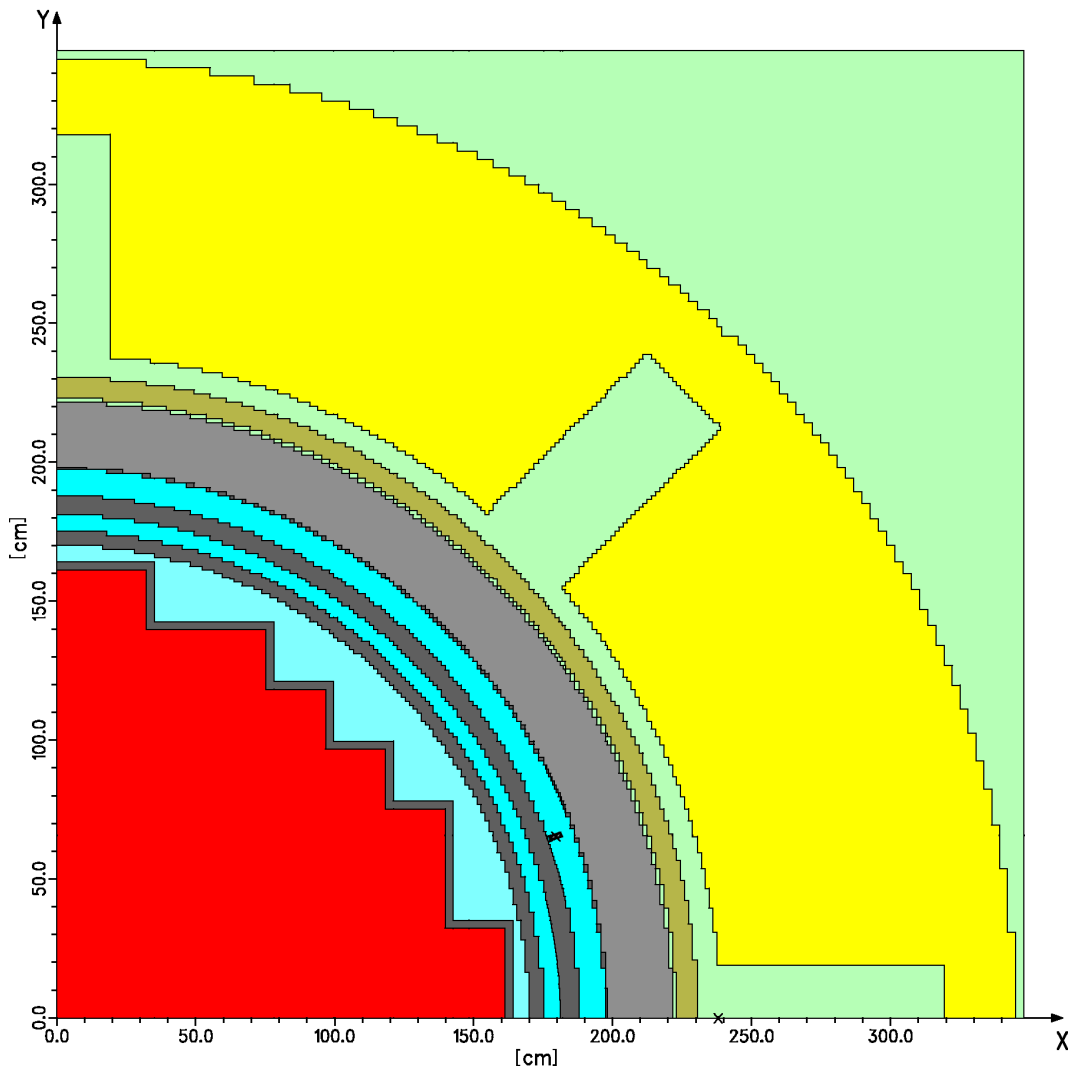
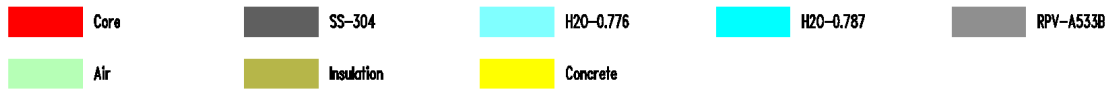


Fig. 4

Compositional and Geometrical Model in the HBR-2 TORT-3.2 (R,θ,Z) Calculations.  
Section at the Core Mid-Plane (Z = 0. cm)

Dosimeter Locations "x", 251R×215θ×103Z Spatial Meshes.

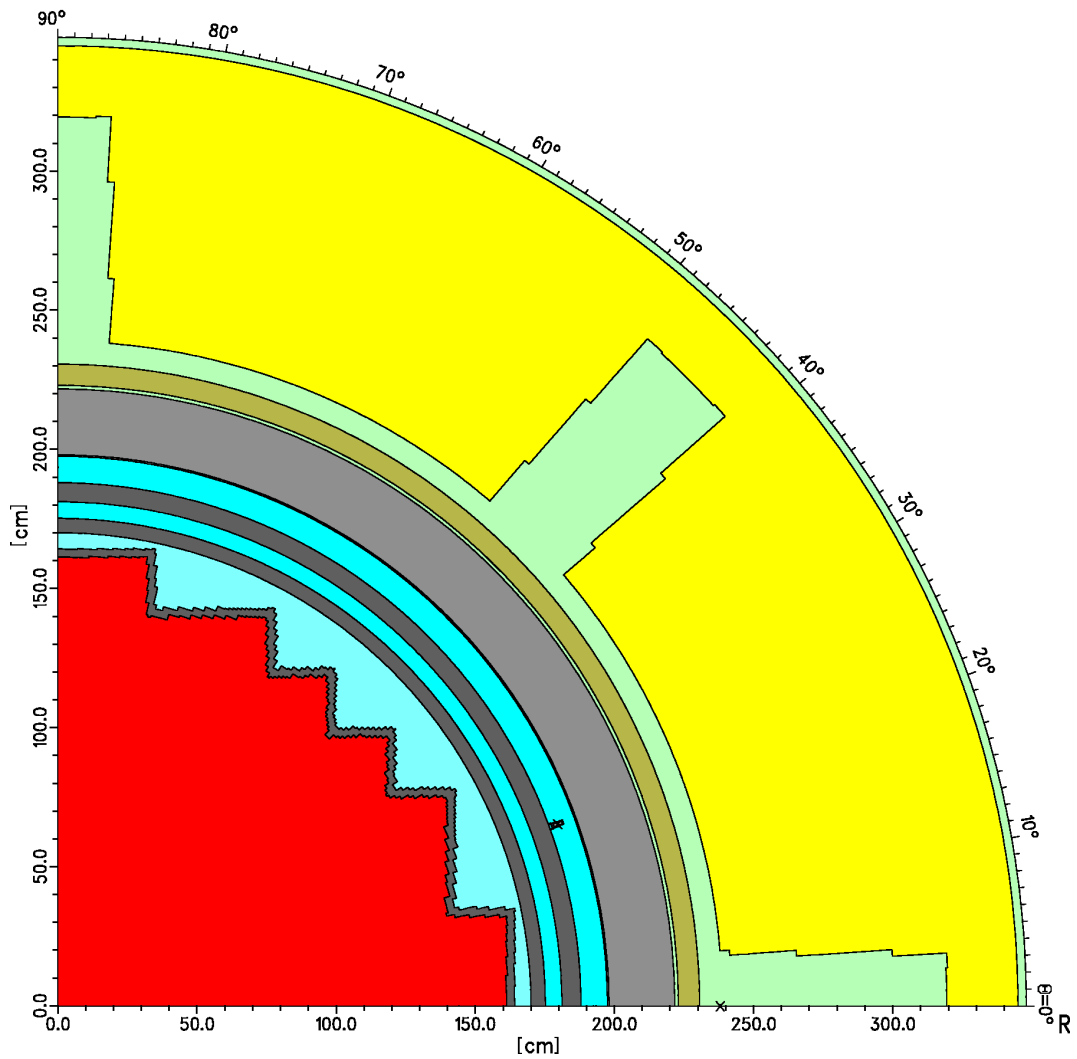
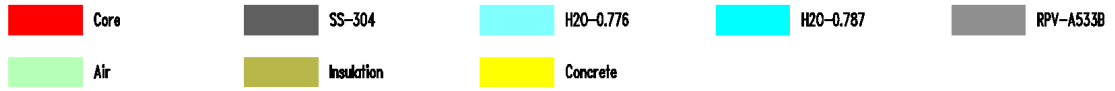




Fig. 5

Zoom on the Capsule Area in the HBR-2 TORT-3.2 (X,Y,Z) Model.  
Section at the Core Mid-Plane (Z = 0. cm)  
Dosimeter Location "x", 255X×240Y×103Z Spatial Meshes.

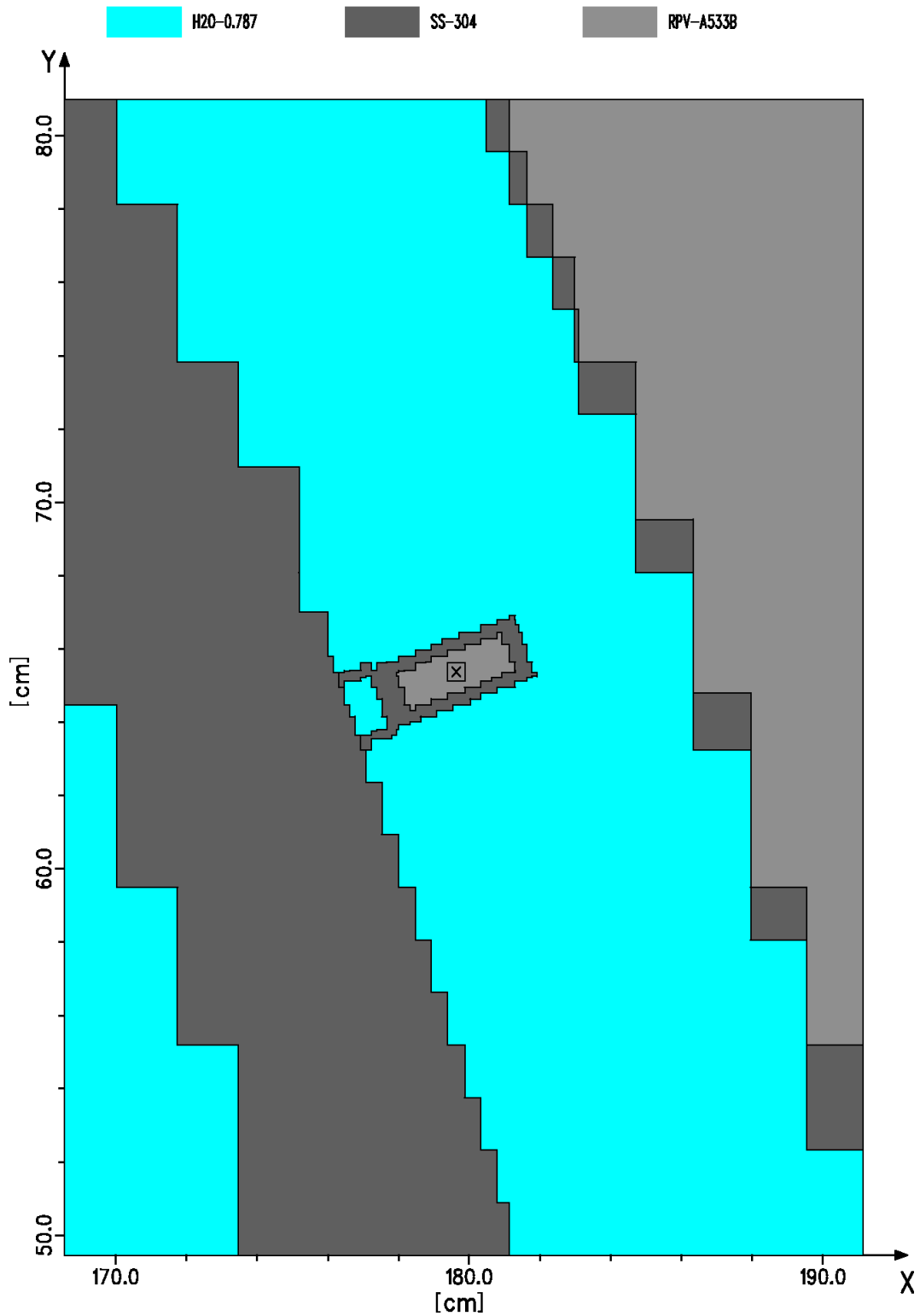


Fig. 6

Zoom on the Capsule Area in the HBR-2 TORT-3.2 (R, $\theta$ ,Z) Model.  
 Section at the Core Mid-Plane (Z = 0. cm)

Dosimeter Location "x", 251R $\times$ 215 $\theta$  $\times$ 103Z Spatial Meshes.

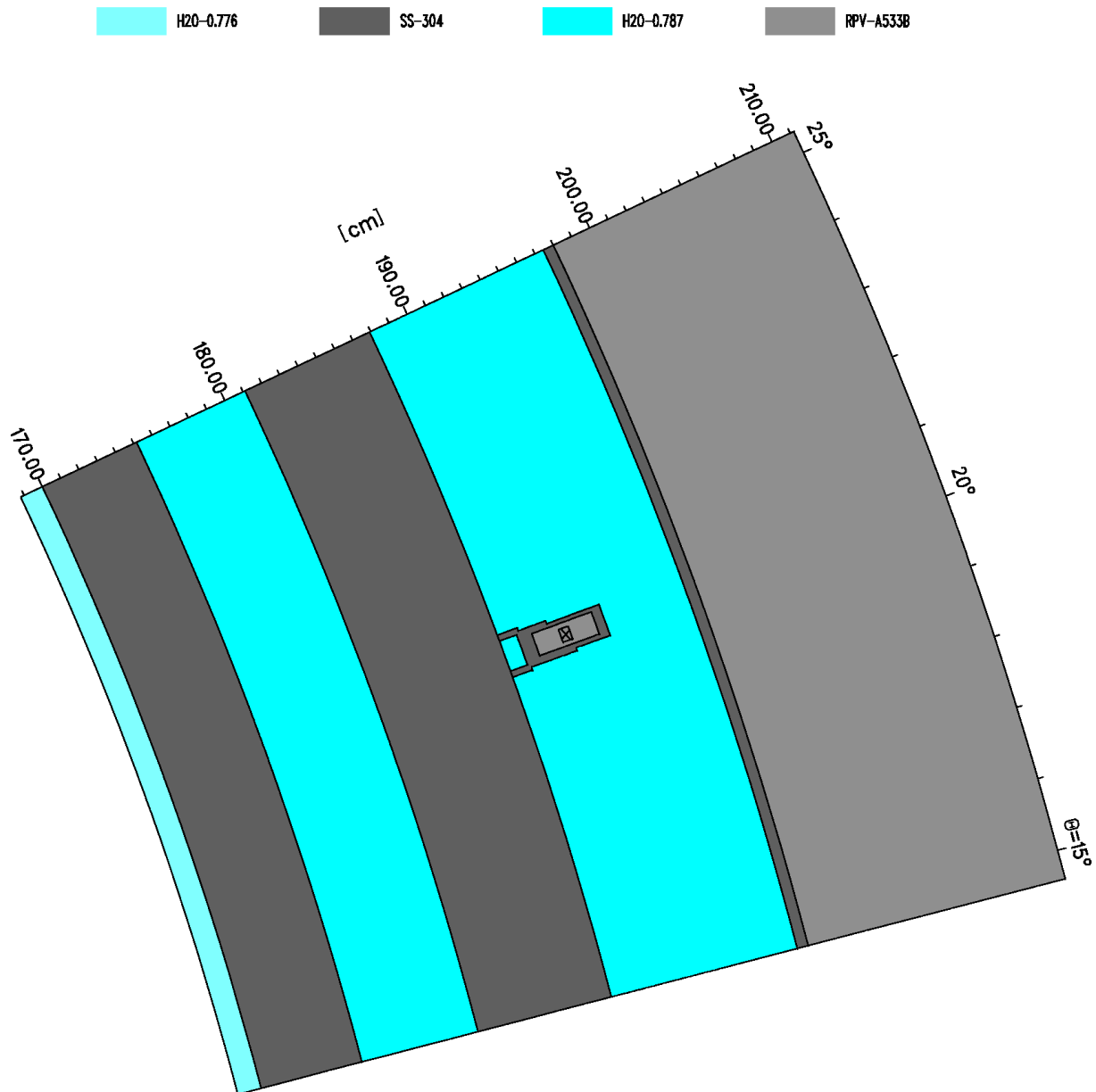


Fig. 7

Zoom on the Normalized Power Density [ $\text{MW}/\text{cm}^3$ ] in the HBR-2 TORT-3.2 (X,Y,Z) Model.  
 [Total Power in the  $\frac{1}{4}$  TORT Model = 0.25 MW]  
 Section at the Core Mid-Plane (Z = 0. cm)  
 255X $\times$ 240Y $\times$ 103Z Spatial Meshes.

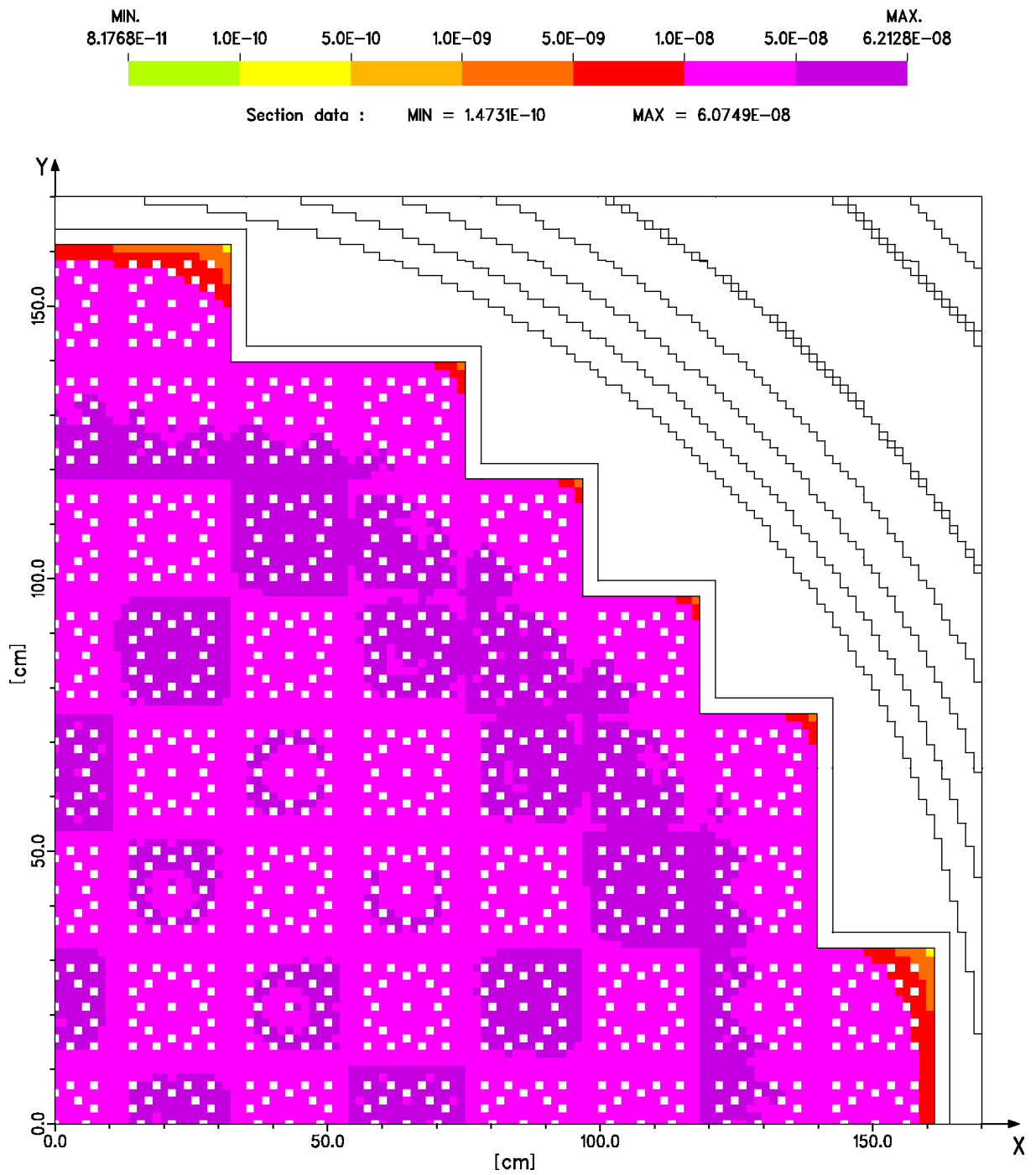
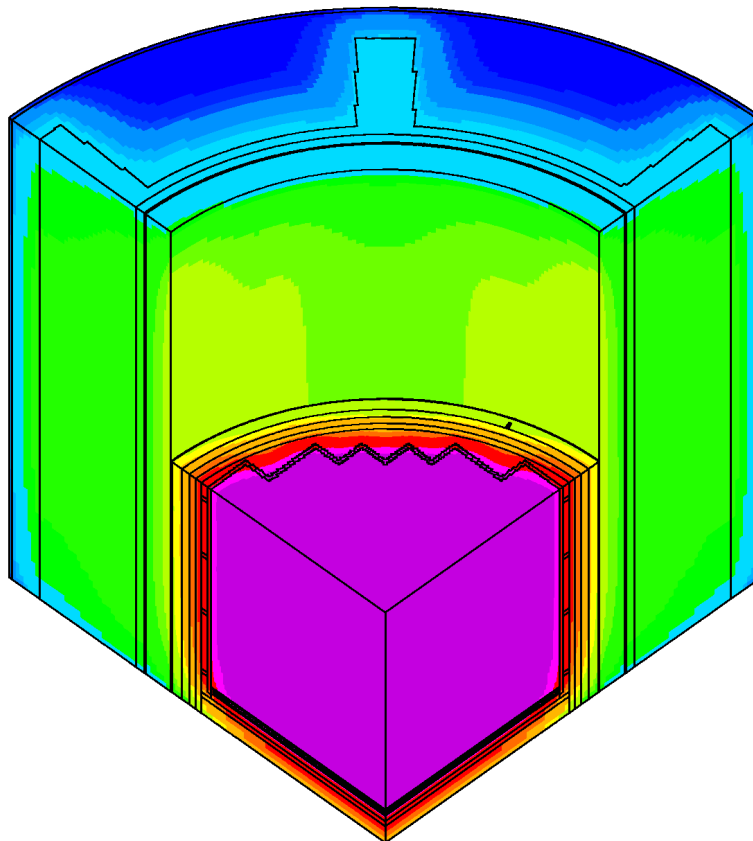
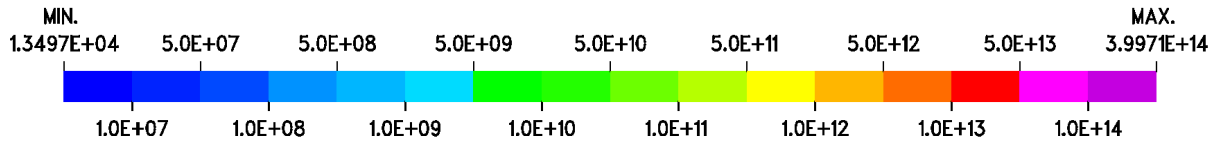


Fig. 8

HBR-2 - Spatial Distribution of the Total Neutron Flux [neutrons $\times$ s $^{-1}\times$ cm $^{-2}$ ].  
3-D View of the Upper Part of the Reactor Pressure Vessel from the Core Mid-Plane.  
251R $\times$ 215 $\theta$  $\times$ 103Z Spatial Meshes.  
P $_3$ -S $_8$  TORT-3.2 (R, $\theta$ ,Z) Calculation Using the BUGJEFF311.BOLIB Library.

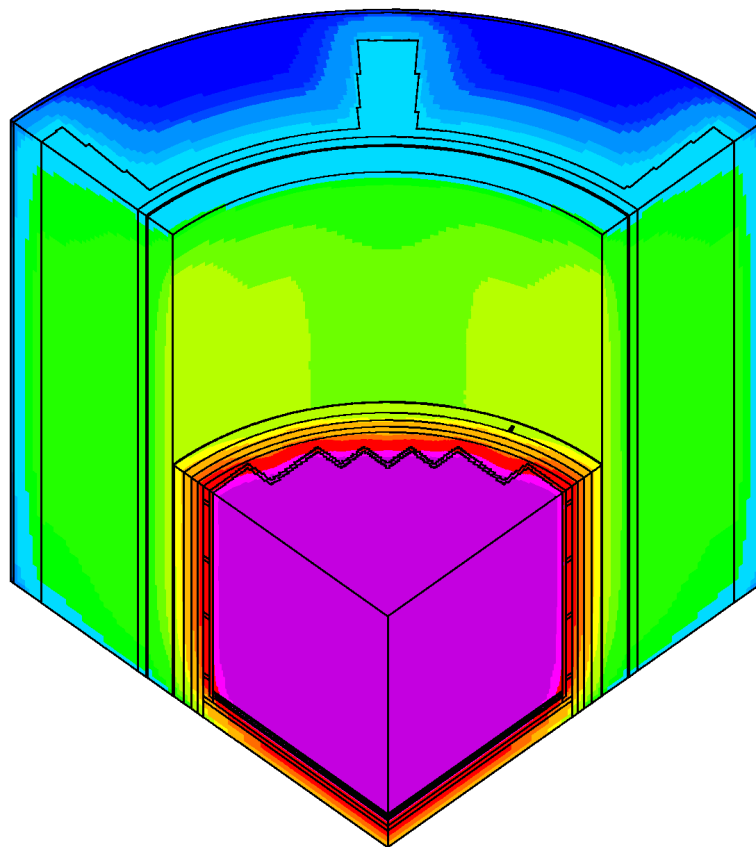
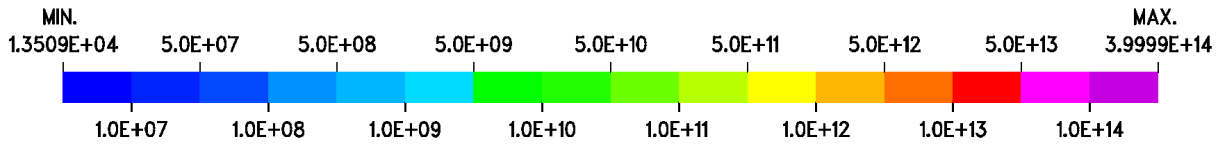


Meshes: 251R,215 $\theta$ ,103Z

$\alpha = 225.00$   $\omega = 45.00$   $R = (0.000E+00, 3.480E+02)$   $\theta = (0.000E+00, 9.000E+01)$   $Z = (-2.135E+02, 2.124E+02)$

Fig. 9

HBR-2 - Spatial Distribution of the Total Neutron Flux [neutrons $\times$ s $^{-1}\times$ cm $^{-2}$ ].  
3-D View of the Upper Part of the Reactor Pressure Vessel from the Core Mid-Plane.  
251R $\times$ 215 $\theta$  $\times$ 103Z Spatial Meshes.  
P $_3$ -S $_8$  TORT-3.2 (R, $\theta$ ,Z) Calculation Using the BUGENDF70.BOLIB Library.



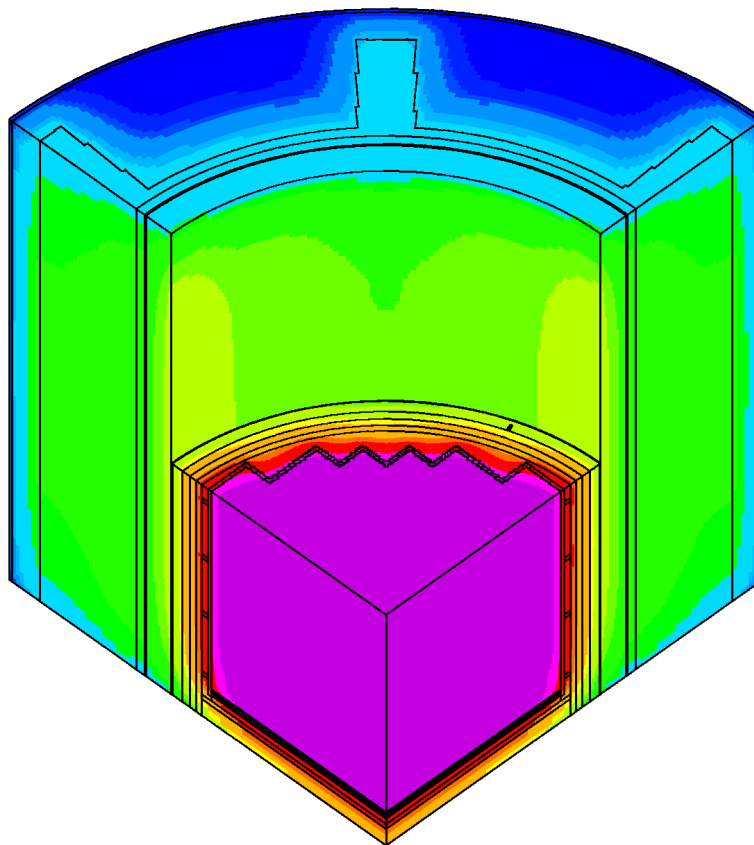
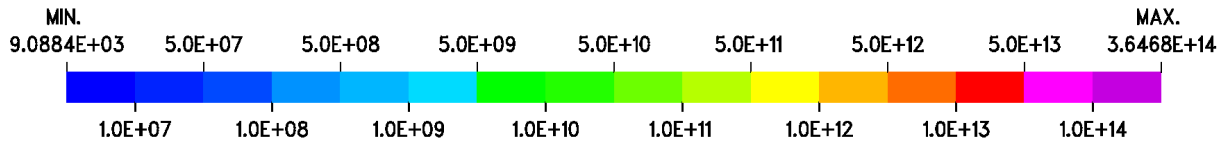
Meshes: 251R,215 $\theta$ ,103Z

$\alpha = 225.00$   $\omega = 45.00$   $R = (0.000E+00, 3.480E+02)$   $\theta = (0.000E+00, 9.000E+01)$   $Z = (-2.135E+02, 2.124E+02)$



Fig. 10

HBR-2 - Spatial Distribution of the Total Neutron Flux [ $\text{neutrons} \times \text{s}^{-1} \times \text{cm}^{-2}$ ].  
3-D View of the Upper Part of the Reactor Pressure Vessel from the Core Mid-Plane.  
251R $\times$ 215 $\theta$  $\times$ 103Z Spatial Meshes.  
P<sub>3</sub>-S<sub>8</sub> TORT-3.2 (R, $\theta$ ,Z) Calculation Using the BUGLE-B7 Library.

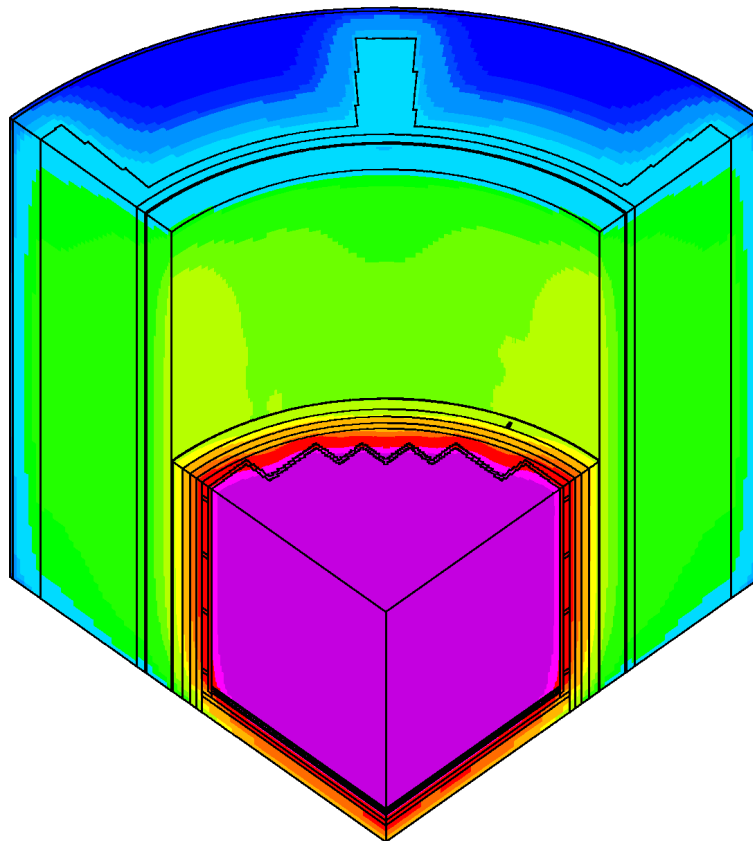
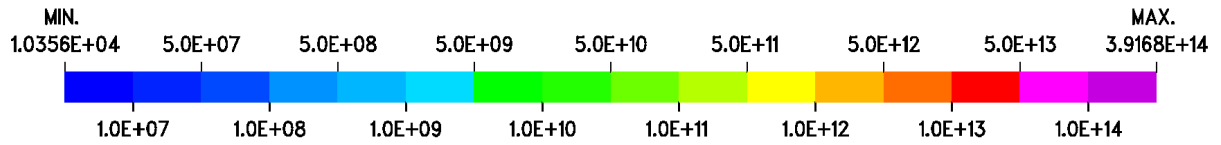


Meshes: 251R,215 $\theta$ ,103Z

$\alpha = 225.00$     $\omega = 45.00$     $R = (0.000E+00, 3.480E+02)$     $\theta = (0.000E+00, 9.000E+01)$     $Z = (-2.135E+02, 2.124E+02)$

Fig. 11

HBR-2 - Spatial Distribution of the Total Neutron Flux [ $\text{neutrons} \times \text{s}^{-1} \times \text{cm}^{-2}$ ].  
 3-D View of the Upper Part of the Reactor Pressure Vessel from the Core Mid-Plane.  
 251R $\times$ 215 $\theta$  $\times$ 103Z Spatial Meshes.  
 P<sub>3</sub>-S<sub>8</sub> TORT-3.2 (R, $\theta$ ,Z) Calculation Using the BUGLE-96 Library.



Meshes: 251R,215 $\theta$ ,103Z

$\alpha = 225.00$     $\omega = 45.00$     $R = (0.000E+00, 3.480E+02)$     $\theta = (0.000E+00, 9.000E+01)$     $Z = (-2.135E+02, 2.124E+02)$

Fig. 12

HBR-2 - P<sub>3</sub>-S<sub>8</sub> TORT-3.2 (R,θ,Z) Calculation.  
Group Flux Ratio - BUGJEFF311.BOLIB to BUGLE-96 Results.

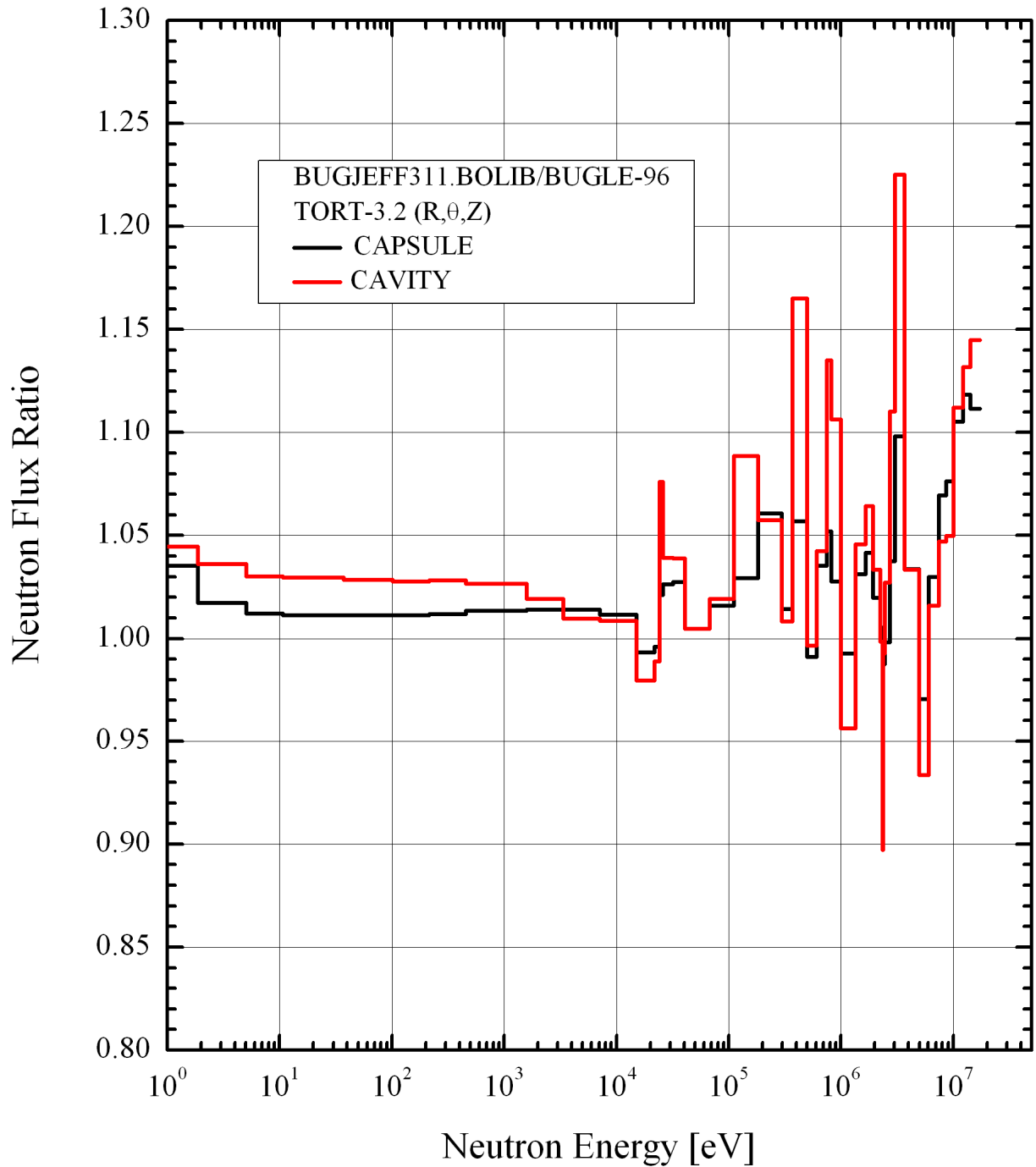


Fig. 13

HBR-2 - P<sub>3</sub>-S<sub>8</sub> TORT-3.2 (R,θ,Z) Calculation.  
Group Flux Ratio - BUGENDF70.BOLIB to BUGLE-96 Results.

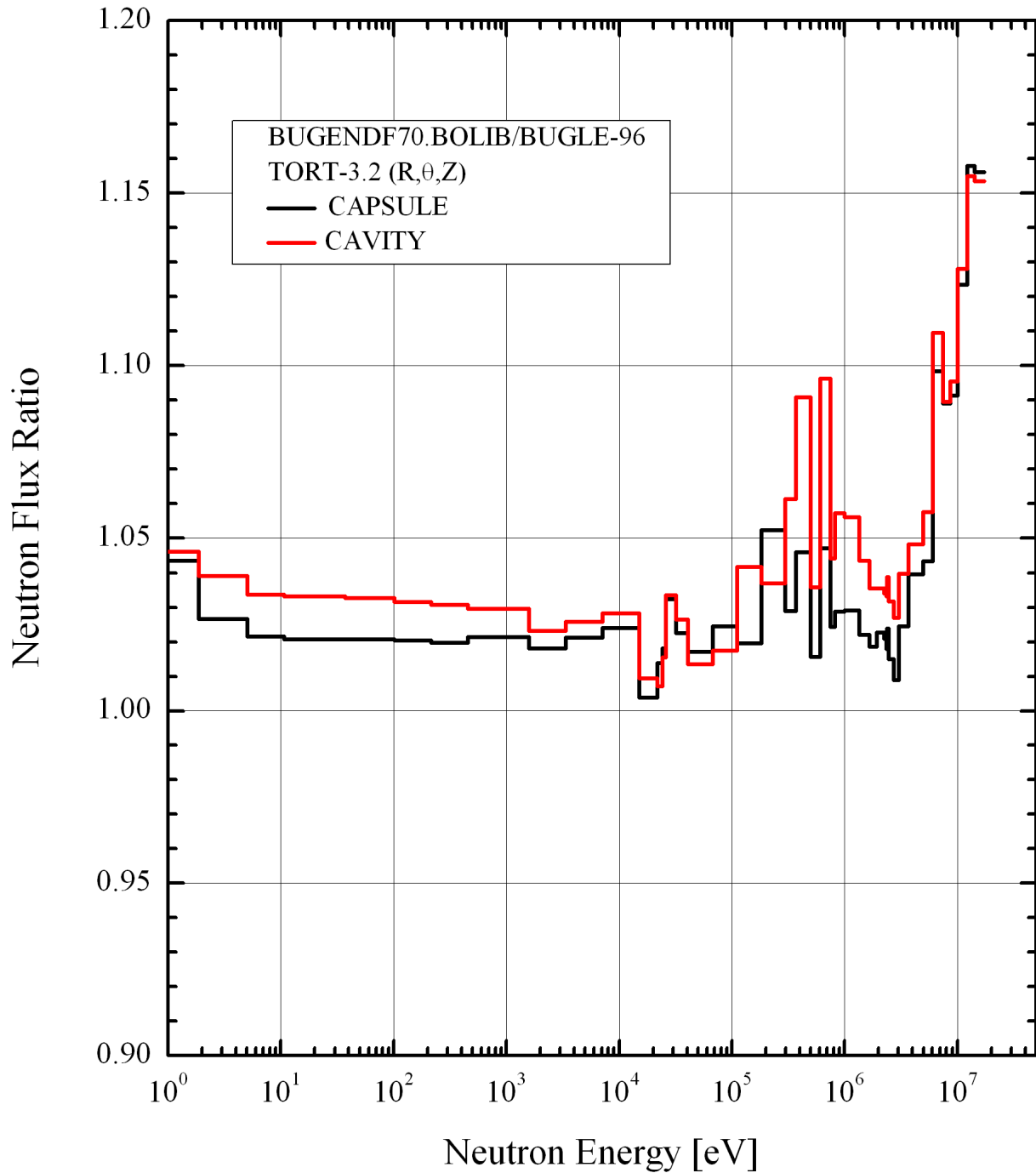


Fig. 14

HBR-2 - P<sub>3</sub>-S<sub>8</sub> TORT-3.2 (R,θ,Z) Calculation.  
Group Flux Ratio - BUGLE-B7 to BUGLE-96 Results.

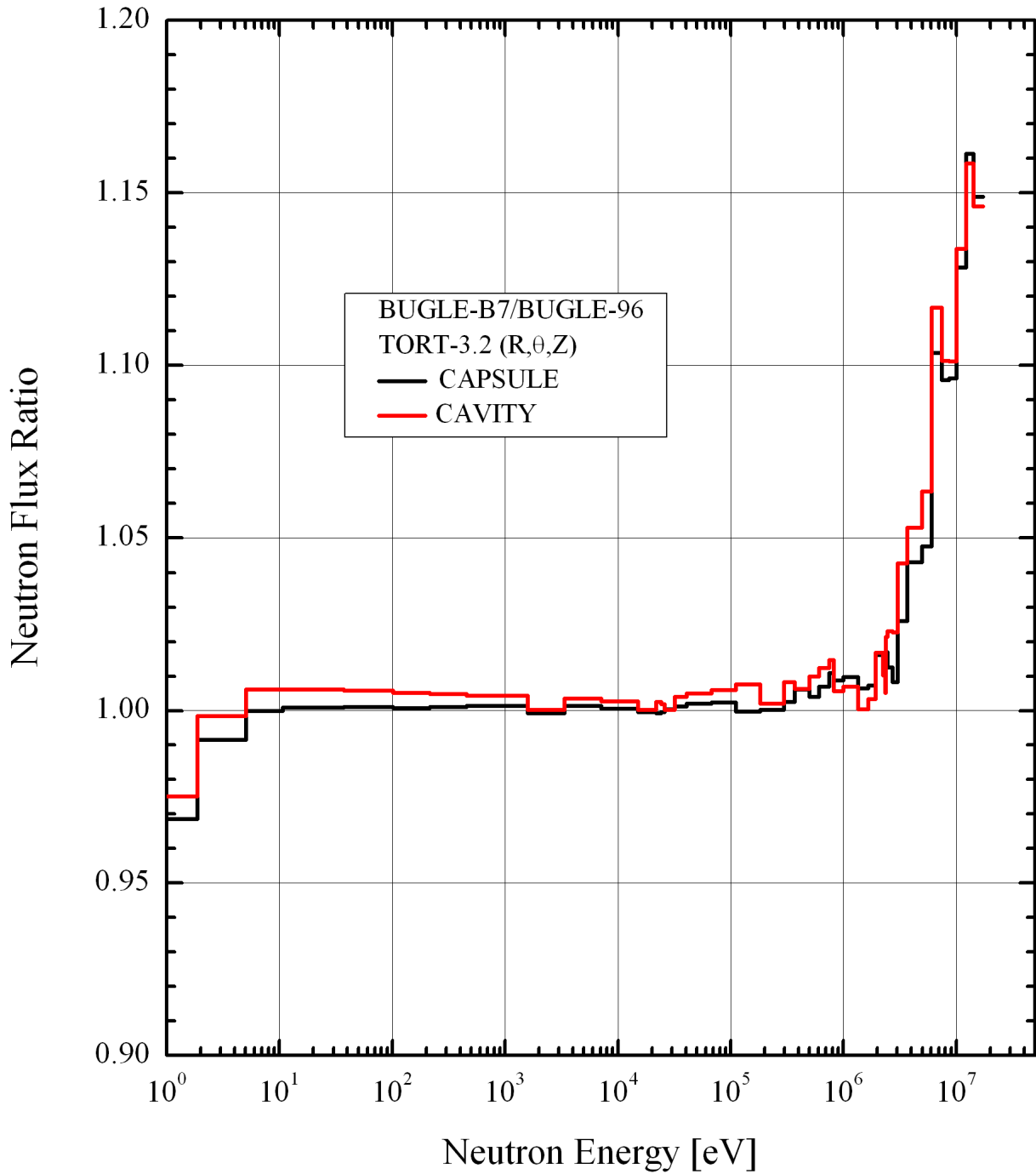




Fig. 15

HBR-2 - P<sub>3</sub>-S<sub>8</sub> TORT-3.2 (R,θ,Z) Calculation.  
Group Flux Ratio - BUGENDF70.BOLIB to BUGLE-B7 Results.

